

# Inverse Bridge Matching Distillation

Nikita Gushchin<sup>1</sup> David Li<sup>\*1</sup> Daniil Selikhanovych<sup>\*123</sup> Evgeny Burnaev<sup>14</sup> Dmitry Baranchuk<sup>2</sup>  
Alexander Korotin<sup>14</sup>

## Abstract

Learning diffusion bridge models is easy; making them fast and practical is an art. Diffusion bridge models (DBMs) are a promising extension of diffusion models for applications in image-to-image translation. However, like many modern diffusion and flow models, DBMs suffer from the problem of slow inference. To address it, we propose a novel distillation technique based on the inverse bridge matching formulation and derive the tractable objective to solve it in practice. Unlike previously developed DBM distillation techniques, the proposed method can distill both conditional and unconditional types of DBMs, distill models in a one-step generator, and use only the corrupted images for training. We evaluate our approach for both conditional and unconditional types of bridge matching on a wide set of setups, including super-resolution, JPEG restoration, sketch-to-image, and other tasks, and show that our distillation technique allows us to accelerate the inference of DBMs from 4x to 100x and even provide better generation quality than used teacher model depending on particular setup.

## 1. Introduction

Diffusion Bridge Models (DBMs) represent a specialized class of diffusion models designed for data-to-data tasks, such as image-to-image translation. Unlike standard diffusion models, which operate by mapping noise to data (Ho et al., 2020; Sohl-Dickstein et al., 2015), DBMs construct diffusion processes directly between two data distributions (Peluchetti, 2023a; Liu et al., 2022b; Somnath et al., 2023; Zhou et al., 2024a; Yue et al., 2024; Shi et al., 2023; De Bortoli et al., 2023). This approach allows DBMs to modify only the necessary components of the data, starting from an input sample rather than generating it entirely from Gaus-

<sup>\*</sup>Equal contribution <sup>1</sup>Skolkovo Institute of Science and Technology <sup>2</sup>Yandex Research <sup>3</sup>HSE University <sup>4</sup>Artificial Intelligence Research Institute. Correspondence to: Nikita Gushchin <n.gushchin@skoltech.ru>, Alexander Korotin <a.korotin@skoltech.ru>.

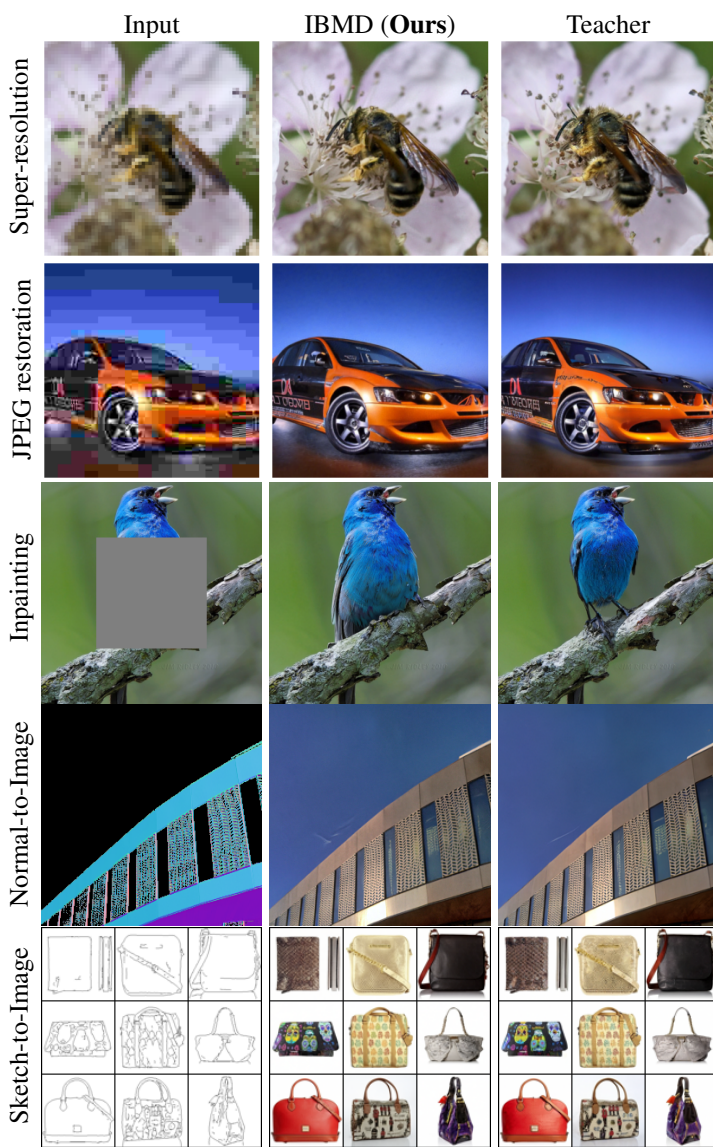


Figure 1. Outputs of DBMs models distilled by our **Inverse Bridge Matching Distillation (IBMD)** approach on various image-to-image translation tasks and datasets (§5). Teachers use  $NFE \geq 500$  steps, while IBMD distilled models use  $NFE \leq 4$ .

sian noise. As a result, DBMs have demonstrated impressive performance in image-to-image translation problems.

The rapid development of DBMs has led to two dominant approaches, usually considered separately. The first branch of

approaches (Peluchetti, 2023a; Liu et al., 2022b; 2023a; Shi et al., 2023; Somnath et al., 2023) considered the construction of diffusion between two arbitrary data distributions performing **Unconditional Bridge Matching** (also called the Markovian projection) of a process given by a mixture of diffusion bridges. The application of this branch includes different data like images (Liu et al., 2023a; Li et al., 2023), audio (Kong et al., 2025) and biological tasks (Somnath et al., 2023; Tong et al., 2024) not only in paired but also in unpaired setups using its relation to the Schrödinger Bridge problem (Shi et al., 2023; Gushchin et al., 2024). The second direction follows a framework closer to classical diffusion models, using forward diffusion to gradually map to the point of different distribution rather than mapping distribution to distribution as in previous case (Zhou et al., 2024a; Yue et al., 2024). While these directions differ in theoretical formulation, their practical implementations are closely related; for instance, models based on forward diffusion can be seen as performing **Conditional Bridge Matching** with additional drift conditions (De Bortoli et al., 2023).

Similar to classical DMs, DBMs also exhibit multistep sequential inference, limiting their adoption in practice. Despite the impressive quality shown by DBMs in the practical tasks, only a few approaches were developed for their acceleration, including more advanced sampling schemes (Zheng et al., 2024; Wang et al., 2024) and consistency distillation (He et al., 2024), adapted for bridge models. While these approaches significantly improve the efficiency of DBMs, some unsolved issues remain. The first one is that the mentioned acceleration approaches are directly applicable only for DBMs based on the Conditional Bridge Matching, i.e., no universal method can accelerate any DBMs. Also, due to some specific theoretical aspects of DBMs, consistency distillation cannot be used to obtain the single-step model (He et al., 2024, Section 3.4).

**Contributions.** To address the above-mentioned issues of DBMs acceleration, we propose a new distillation technique based on the inverse bridge matching problem, which has several advantages compared to existing methods:

1. **Universal Distillation.** Our distillation technique is applicable to DBMs trained with both conditional and unconditional regimes, making it the first distillation approach introduced for unconditional DBMs.
2. **Single-Step and Multistep Distillation.** Our distillation is capable of distilling DBMs into generators with any specified number of steps, including the distillation of DBMs into one-step generators.
3. **Target data-free distillation.** Our method does not require the target data domain to perform distillation.
4. **Better quality of distilled models.** Our distillation technique is tested on a wide set of image-to-image problems

for conditional and unconditional DBMs in both one and multi-step regimes. It demonstrates improvements compared to the previous acceleration approaches including DBIM (Zheng et al., 2024) and CDBM (He et al., 2024).

## 2. Background

In this paper, we propose a universal distillation framework for both conditional and unconditional DBMs. To not repeat fully analogical results for both cases, we denote by **this color the additional conditioning on  $x_T$**  used for the conditional models, i.e. for the unconditional case this conditioning is not used.

### 2.1. Bridge Matching

We start by recalling the bridge matching method (Peluchetti, 2023b;a; Liu et al., 2022b; Shi et al., 2023). Consider two probability distributions  $p(x_0)$  and  $p(x_T)$  on  $\mathbb{R}^D$  dimensional space, which represent target and source domains, respectively. For example, in an image inverse problem,  $p(x_0)$  represents the distribution of *clean* images and  $p(x_T)$  the distribution of *corrupted* images. Also consider a coupling  $p(x_0, x_T)$  of these two distributions, which is a probability distribution on  $\mathbb{R}^D \times \mathbb{R}^D$ . Coupling  $p(x_0, x_T)$  can be provided by paired data or constructed synthetically, i.e., just using the independent distribution  $p(x_0, x_T) = p(x_0)p(x_T)$ . Bridge Matching aims to construct the diffusion that transforms source distribution  $p(x_T)$  to target distribution  $p(x_0)$  based on given coupling  $p(x_0, x_T)$  and specified *diffusion bridge*.

**Diffusion bridges.** Consider forward-time diffusion  $Q$  called "Prior" on time horizon  $[0, T]$  represented by the stochastic differential equation (SDE):

$$\text{Prior } Q : \quad dx_t = f(x_t, t)dt + g(t)dw_t, \quad (1)$$

$$f(x_t, t) : \mathbb{R}^D \times [0, T] \rightarrow \mathbb{R}^D, \quad g(t) : [0, T] \rightarrow \mathbb{R}^D,$$

where  $f(x_t, t)$  is a drift function,  $g(t)$  is the noise schedule function and  $dw_t$  is the differential of the standard Wiener process. By  $q(x_t|x_s)$ , we denote the transition probability density of prior process  $Q$  from time  $s$  to time  $t$ . *Diffusion bridge* is a conditional process  $Q_{|x_0, x_T}$ , which is obtained by pinning down starting and ending points  $x_0$  and  $x_T$ . This diffusion bridge can be derived from prior process  $Q$  using the Doob-h transform (Doob & Doob, 1984):

$$\text{Diffusion Bridge } Q_{|x_0, x_T} : x_0, x_T \text{ are fixed}, \quad (2)$$

$$dx_t = \{f(x_t, t)dt + g^2(t)\nabla_{x_t} \log q(x_T|x_t)\}dt + g(t)dw_t,$$

For this diffusion bridge we denote the distribution at time  $t$  of the diffusion bridge  $Q_{|x_0, x_T}$  by  $q(x_t|x_0, x_T)$ .

**Mixture of bridges.** Bridge Matching procedure starts with creating a *mixture of bridges* process  $\Pi$ . This process is

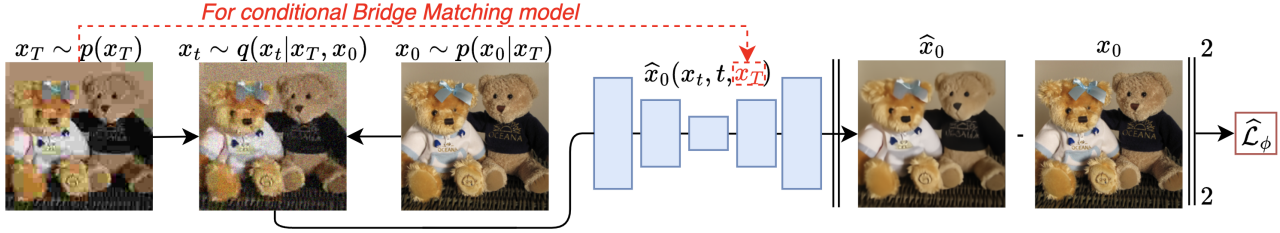


Figure 2. **Overview of (Conditional) Bridge Matching with  $\hat{x}_0$  reparameterization.** The process begins by sampling a pair  $(x_0, x_T)$  from the data coupling  $p(x_0, x_T)$ . An intermediate sample  $x_t$  is then drawn from the diffusion bridge  $q(x_t|x_0, x_T)$  at a random time  $t \sim U[0, T]$ . The model  $\hat{x}_0$  is trained with an MSE loss to reconstruct  $x_0$  from  $x_t$ . In the conditional setting (dashed red path),  $\hat{x}_0$  is also conditioned on  $x_T$  as an additional input, leveraging information about the terminal state to improve reconstruction.

represented as follows:

Mixture of Bridges  $\Pi$  :

$$\Pi(\cdot) = \int Q_{|x_0, x_T}(\cdot) p(x_0, x_T) dx_0 dx_T. \quad (3)$$

Practically speaking, the definition (3) means that to sample from a mixture of bridges  $\Pi$ , one first samples the pair  $(x_0, x_T) \sim p(x_0, x_T)$  from data coupling and then samples trajectory from the bridge  $Q_{|x_0, x_T}(\cdot)$ .

**Bridge Matching problem.** The mixture of bridges  $\Pi$  cannot be used for data-to-data translation since it requires first to sample a pair of data and then just inserts the trajectory. In turn, we are interested in constructing a diffusion, which can start from any sample  $x_T \sim p(x_T)$  and gradually transform it to  $x_0 \sim p(x_0)$ . This can be done by solving the Bridge Matching problem (Shi et al., 2023, Proposition 2)

*Bridge Matching problem:* (4)

$$\text{BM}(\Pi) \stackrel{\text{def}}{=} \arg \min_{M \in \mathcal{M}} \text{KL}(\Pi || M),$$

where  $\mathcal{M}$  is the set of Markovian processes associated with some SDE and  $\text{KL}(\Pi || M)$  is the KL-divergence between a constructed mixture of bridges  $\Pi$  and diffusion  $M$ . It is known that the solution of Bridge Matching is the reversed-time SDE (Shi et al., 2023, Proposition 9):

*The SDE of Bridge Matching solution :* (5)

$$dx_t = \{f_t(x_t) - g^2(t)v^*(x_t, t)\}dt + g(t)d\bar{w}_t, \\ x_T \sim p_T(x_T),$$

where  $\bar{w}$  is a standard Wiener process when time  $t$  flows backward from  $t = T$  to  $t = 0$ , and  $dt$  is an infinitesimal negative timestep. The drift function  $v^*$  is obtained solving the following problem (Shi et al., 2023; Liu et al., 2023a):

*Bridge Matching problem with a tractable objective:* (6)

$$\min_{\phi} \mathbb{E}_{x_0, t, x_t} [\|v_{\phi}(x_t, t) - \nabla_{x_t} \log q(x_t|x_0)\|^2], \\ (x_0, x_T) \sim p(x_0, x_T), t \sim U([0, T]), x_t \sim q(x_t|x_0, x_T).$$

Time moment  $t$  here is sampled according to the uniform distribution on the interval  $[0, T]$ .

**Relation Between Flow and Bridge Matching.** The Flow Matching (Liu et al., 2023b; Lipman et al., 2023) can be seen as the limiting case  $\sigma \rightarrow 0$  of the Bridge Matching for particular example see (Shi et al., 2023, Appendix A.1).

## 2.2. Augmented (Conditional) Bridge Matching and Denoising Diffusion Bridge Models (DDBM)

For a given coupling  $p(x_0, x_T) = p(x_0|x_T)p(x_T)$ , one can use an alternative approach to build a data-to-data diffusion. Consider a set of Bridge Matching problems indexed by  $x_T$  between  $p_0 = p(x_0|x_T)$  and  $p(x_T) = \delta_{x_T}(x)$  (delta measure centered at  $x_T$ ). This approach is called Augmented Bridge Matching (De Bortoli et al., 2023). The key difference of this version in practice is that it introduces the condition of the drift function  $v^*(x_t, t, x_T)$  on the starting point  $x_T$  in the reverse time diffusion (5):

$$dx_t = \{f_t(x_t) - g^2(t)v^*(x_t, t, x_T)\}dt + g(t)d\bar{w}_t.$$

The drift function  $v^*$  can be recovered almost in the same way just by the addition of this condition on  $x_T$ :

*Augmented (Conditional) Bridge Matching Problem.*

$$\min_{\phi} \mathbb{E}_{x_0, t, x_t, x_T} [\|v_{\phi}(x_t, t, x_T) - \nabla_{x_t} \log q(x_t|x_0)\|^2], \\ (x_0, x_T) \sim p(x_0, x_T), \text{ and } x_t \sim q(x_t|x_0, x_T).$$

Since the difference is the addition of conditioning on  $x_T$ , we call this approach *Conditional Bridge Matching*.

**Relation to DDBM.** As was shown in the Augmented Bridge Matching (De Bortoli et al., 2023), the conditional Bridge Matching is equivalent to the Denoising Diffusion Bridge Model (DDBM) proposed in (Zhou et al., 2024a). The difference is that in DDBM, the authors learn the score function of  $s(x_t, x_T, t)$  conditioned on  $x_T$  of a process for which  $x_0 \sim p(x_0|x_T)$  and  $q(x_t) \sim q(x_t|x_0, x_T)$ : Then, it is combined with the drift of forward Doob-h transform (5) to get the reverse SDE drift  $v(x_t, t, x_T)$ :

$$v(x_t, t, x_T) = s(x_t, x_T, t) - \nabla_{x_t} \log q(x_T|x_t), \\ dx_t = \{f(x_t, t)dt - g^2(t)v(x_t, t, x_T)\}dt + g(t)d\bar{w}_t,$$

or reverse probability flow ODE drift:

$$v_{\text{ODE}}(x_t, t, x_T) = \frac{1}{2}s(x_t, x_T, t) - \nabla_{x_t} \log q(x_T|x_t),$$

$$dx_t = \{f(x_t, t)dt - g^2(t)v_{\text{ODE}}(x_t, t, x_T)\}dt,$$

which is used for consistency distillation in (He et al., 2024).

### 2.3. Practical aspects of Bridge Matching

**Priors used in practice.** In practice (He et al., 2024; Zhou et al., 2023; Zheng et al., 2024), the drift of the prior process is usually set to be  $f(x_t, t) = f(t)x_t$ , i.e, it depends linearly on  $x_t$ . For this process the transitional distribution  $q(x_t|x_0) = \mathcal{N}(x_t|\alpha_t x_0, \sigma_t^2 I)$  is Gaussian, where:

$$f(t) = \frac{d \log \alpha_t}{dt}, \quad g^2(t) = \frac{d\sigma_t^2}{dt} - 2\frac{d \log \alpha_t}{dt} \sigma_t^2.$$

The bridge process distribution is also a Gaussian  $q(x_t|x_0, x_T) = \mathcal{N}(x_T|a_t x_T + b_t x_0, c_t^2 I)$  with coefficients:

$$a_t = \frac{\alpha_t}{\alpha_T} \frac{\text{SNR}_T}{\text{SNR}_t}, \quad b_t = \alpha_t \left(1 - \frac{\text{SNR}_T}{\text{SNR}_t}\right), \\ c_t^2 = \sigma_t^2 \left(1 - \frac{\text{SNR}_T}{\text{SNR}_t}\right),$$

where  $\text{SNR}_t = \frac{\alpha_t^2}{\sigma_t^2}$  is the signal-to-noise ratio at time  $t$ .

**Data prediction reparameterization.** The regression target of the loss function (6) for the priors with the drift  $v(x_t, t)$  is given by  $\nabla_{x_t} \log q(x_t|x_0) = -\frac{x_t - \alpha_t x_0}{\sigma_t^2}$ . Hence, one can use the parametrization  $v(x_t, t, x_T) = -\frac{x_t - \alpha_t \hat{x}_0(x_t, t, x_T)}{\sigma_t^2}$  and solve the equivalent problem:

*Reparametrized (Conditional) Bridge Matching problem:*

$$\min_{\phi} \mathbb{E}_{x_0, t, x_t, x_T} [\lambda(t) \|\hat{x}_0^\phi(x_t, t, x_T) - x_0\|^2], \quad (7)$$

$$(x_0, x_T) \sim p(x_0, x_T), \quad t \sim U([0, T]), \quad x_t \sim q(x_t|x_0, x_T),$$

where  $\lambda(t)$  is any positive weighting function. Note that  $x_T$  is used only for the Conditional Bridge Matching model.

### 2.4. Difference Between Acceleration of Unconditional and Conditional DBMs

Since both conditional and unconditional approaches learn drifts of SDEs, they share the same problems of long inference. However, these models significantly differ in the approaches that can accelerate them. The source of this difference is that Conditional Bridge Matching considers the set of problems of reversing diffusion, which gradually transforms distribution  $p(x_0|x_T)$  to the fixed point  $x_T$ . Furthermore, the forward diffusion has simple analytical drift and Gaussian transitional kernels. Thanks to it, for each  $x_T$  to sample, one can use the probability flow ODE and ODE-solvers or hybrid solvers to accelerate sampling (Zhou et al., 2024a) or use consistency distillation of bridge models (He et al., 2024). Another beneficial property is that one can consider a non-Markovian forward process to develop a more efficient sampling scheme proposed in DBIM (Zheng et al.,

2024) similar to Denoising Diffusion Implicit Models (Song et al., 2021). However, in the Unconditional Bridge Matching problem, the forward diffusion process, which maps  $p(x_0)$  to  $p(x_T)$  without conditioning on specific point  $x_T$ , is unknown. Hence, the abovementioned methods cannot be used to accelerate this model type.

## 3. IBMD: Inverse Bridge Matching Distillation

This section describes our proposed universal approach to distill the both Unconditional and (Conditional) Bridge Matching models  $v^*$  (called the teacher model) into a few-step generator *using only the corrupted data*  $p_T(x_T)$ . The key idea of our method is to consider the inverse problem of finding the mixture of bridges  $\Pi_\theta$ , for which Bridge Matching provides the solution  $v_\theta$  with the same drift as the given teacher model  $v^*$ . We formulate this task as the optimization problem (§3.1). However, gradient methods cannot solve this optimization problem directly due to the absence of tractable gradient estimation. To avoid this problem, we prove a theorem that allows us to reformulate the inverse problem in the tractable objective for gradient optimization (§3.2). Then, we present the fully analogical results for the Conditional Bridge Matching case in (§3.3). Next, we present the multistep version of distillation (§3.5) and the final algorithm (§3.4). We provide the proofs for all considered theorems and propositions in Appendix A.

### 3.1. Bridge Matching Distillation as Inverse Problem

In this section, we focus on the derivation of our distillation method for the case of Unconditional Bridge Matching. Consider the fitted teacher model  $v^*(x_t, t)$ , which is an SDE drift of some process  $M^* = \text{BM}(\Pi^*)$ , where  $\Pi^*$  constructed using some data coupling  $p^*(x_0, x_T) = p^*(x_0|x_T)p(x_T)$ . We parametrize  $p_\theta(x_0, x_T) = p_\theta(x_0|x_T)p(x_T)$  and aim to find such  $\Pi_\theta$  build on  $p_\theta(x_0, x_T)$ , that  $\text{BM}(\Pi^*) = \text{BM}(\Pi_\theta)$ . In practice, we parametrize  $p_\theta(x_0|x_T)$  by the stochastic generator  $G_\theta(x_T, z)$ ,  $z \sim \mathcal{N}(0, I)$ , which generates samples based on input  $x_T \sim p(x_T)$  and the gaussian noise  $z$ . Now, we formulate the inverse problem as follows:

$$\min_{\theta} \text{KL}(\text{BM}(\Pi_\theta) || M^*). \quad (8)$$

Note, that since the objective (8) is the KL-divergence between  $\text{BM}(\Pi_\theta)$  and  $M^*$ , it is equal to 0 if and only if  $\text{BM}(\Pi_\theta)$  and  $M^*$  coincide. Furthermore, using the disintegration and Girsanov theorem (Vargas et al., 2021; Pavon & Wakolbinger, 1991), we have the following result:

**Proposition 3.1** (Inverse Bridge Matching problem). *The inverse problem (8) is equivalent to*

$$\min_{\theta} \mathbb{E}_{x_t, t} [\lambda(t) \|v(x_t, t) - v^*(x_t, t)\|^2], \quad s.t. \quad (9)$$

$$v = \arg \min_{v'} \mathbb{E}_{x_t, t, x_0} [\|v'(x_t, t) - \nabla_{x_t} \log q(x_t|x_0)\|^2], \\ (x_0, x_T) \sim p_\theta(x_0, x_T), \quad t \sim U([0, T]), \quad x_t \sim q(x_t|x_0, x_T),$$

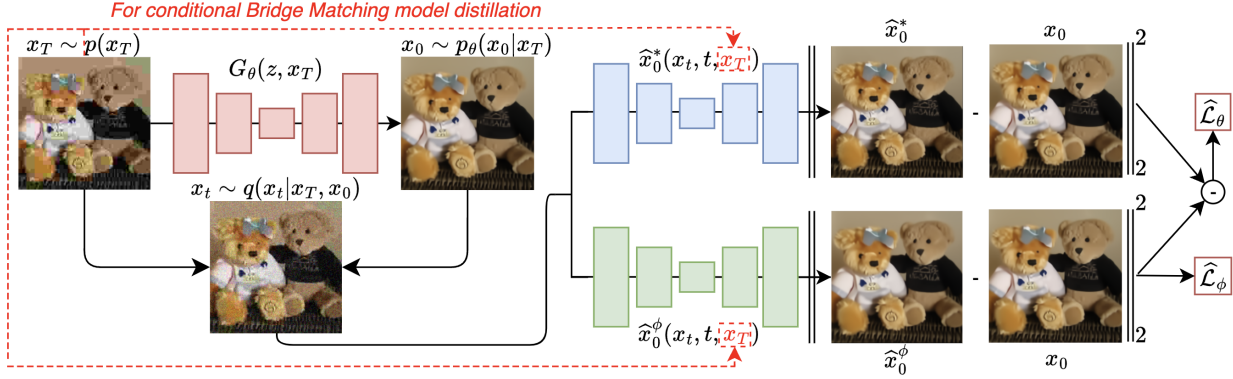


Figure 3. **Overview of our method Inverse Bridge Matching Distillation (IBMD).** The goal is to distill a trained (**Conditional**) Bridge Matching model into a generator  $G_\theta(z, x_T)$ , which learns to produce samples using the corrupted data  $p(x_T)$ . Generator  $G_\theta(z, x_T)$  defines the coupling  $p_\theta(x_0, x_T) = p_\theta(x_0|x_T)p(x_T)$  and we aim to learn the generator in such way that Bridge Matching with  $p_\theta(x_0, x_T)$  produces the same (**Conditional**) Bridge Matching model  $\hat{x}_0^\phi = \hat{x}_0^*$ . To do so, we learn a bridge model  $\hat{x}_0^\phi$  using coupling  $p_\theta$  in the same way as the teacher model was learned. Then, we use our novel objective given in Theorem 3.2 to update the generator model  $G_\theta$ .

where  $\lambda(t)$  is any positive weighting function.

Thus, this is the **constrained** problem, where the drift  $v$  is the result of Bridge Matching for coupling  $p_\theta(x_0, x_T)$  parametrized by the generator  $G_\theta$ . Unfortunately, there is no clear way to use this objective efficiently for optimizing a generator  $G_\theta$  since it would require gradient backpropagation through the argmin of the Bridge Matching problem.

### 3.2. Tractable objective for the inverse problem

In this section, we introduce our new **unconstrained** reformulation for the inverse problem (9), which admits direct optimization using gradient methods:

**Theorem 3.2** (Tractable inverse problem reformulation). *The constrained inverse problem (9) w.r.t  $\theta$  is equivalent to the unconstrained optimization problem:*

$$\begin{aligned} & \min_{\theta} \left[ \mathbb{E}_{x_t, t, x_0} [\lambda(t) \|v^*(x_t, t) - \nabla_{x_t} \log q(x_t|x_0)\|^2] - \right. \\ & \left. \min_{\phi} \mathbb{E}_{x_t, t, x_0} [\lambda(t) \|v_\phi(x_t, t) - \nabla_{x_t} \log q(x_t|x_0)\|^2] \right], \\ & (x_0, x_T) \sim p_\theta(x_0, x_T), t \sim U([0, T]), x_t \sim q(x_t|x_0, x_T), \end{aligned}$$

Where the constraint in the original inverse problem (9) is relaxed by introducing the inner bridge matching problem.

This is the general result that can be applied with any diffusion bridge. For the priors with drift  $f(x_t, t) = f(t)x_t$ , we present its reparameterized version.

**Proposition 3.3** (Reparameterized tractable inverse problem). *Using the reparameterization (§2.3) for the prior with the linear drift  $f(x_t, t) = f(t)x_t$ , the inverse problem in Theorem 3.2 is equivalent to:*

$$\begin{aligned} & \min_{\theta} \left[ \mathbb{E}_{x_t, t, x_0} [\lambda(t) \|\hat{x}_0^*(x_t, t) - x_0\|^2] - \right. \\ & \left. \min_{\phi} \mathbb{E}_{x_t, t, x_0} [\lambda(t) \|\hat{x}_0^\phi(x_t, t) - x_0\|^2] \right], \end{aligned}$$

$$(x_0, x_T) \sim p_\theta(x_0, x_T), t \sim U([0, T]), x_t \sim q(x_t|x_0, x_T).$$

The key difference of the reformulated problem is that it admits clear gradients of generator  $G_\theta$ , which can be calculated automatically by using the autograd techniques. Thanks to the unconstrained reformulation of an inverse problem given by Theorem 3.2, it can now be solved directly by parameterizing  $\hat{x}_0(x_t, t)$  by a neural network.

### 3.3. Distillation of conditional Bridge Matching models

Since Conditional Bridge Matching is, in essence, a set of Unconditional Bridge Matching problems for each  $x_T$  (§2.2), the analogical results hold just by adding the conditioning on  $x_T$  for  $v$ , i.e., using  $v(x_t, t, x_T)$  or  $\hat{x}_0$ , i.e. using  $\hat{x}_0(x_t, t, x_T)$ . Here, we provide the final reparameterized formulation, which we use in our experiments:

**Theorem 3.4** (Reparameterized tractable inverse problem for conditional bridge matching).

$$\begin{aligned} & \min_{\theta} \left[ \mathbb{E}_{x_t, t, x_0, x_T} [\lambda(t) \|\hat{x}_0^*(x_t, t, x_T) - x_0\|^2] - \right. \\ & \left. \min_{\phi} \mathbb{E}_{x_t, t, x_0, x_T} [\lambda(t) \|\hat{x}_0^\phi(x_t, t, x_T) - x_0\|^2] \right], \\ & (x_0, x_T) \sim p_\theta(x_0, x_T), t \sim U([0, T]), x_t \sim q(x_t|x_0, x_T). \end{aligned} \quad (10)$$

where  $\lambda(t)$  is some positive weight function.

To use it in practice, we parameterize  $\hat{x}_0(x_t, t, x_T)$  by a neural network with an additional condition on  $x_T$ .

### 3.4. Algorithm

We provide a one-step Algorithm 1 that solves the inverse Bridge Matching problem in the reformulated version that we use in our experiments. We provide a visual abstract of it in Figure 3. Note that a teacher in the velocity parameterization  $v^*(x_t, t)$  can be easily reparameterized (§2.3) in  $x_0$ -prediction model using  $\hat{x}^*(x_t, t) = \frac{\sigma_t^2 v^*(x_t, t) + x_t}{\alpha_t}$ .

### 3.5. Multistep distillation

We also present a multistep modification of our distillation technique if a one-step generator struggles to distill the models, e.g., in inpainting setups, where the corrupted image  $x_T$  contains less information. Our multistep technique is inspired by similar approaches used in diffusion distillation methods (Yin et al., 2024a, DMD) and aims to avoid training/inference distribution mismatch.

We choose  $N$  timesteps  $\{0 < t_1 < t_2 < \dots < t_N = T\}$  and add additional time input to our generator  $G_\theta(x_t, z, t)$ . For the conditional Bridge Matching case, we also add conditions on  $x_T$  and use  $G_\theta(x_t, z, t, x_T)$ . To perform inference, we alternate between getting prediction from the generator  $\tilde{x}_0 = G_\theta(x_t, z, t)$  and using posterior sampling  $q(x_{t_{n-1}}|\tilde{x}_0, x_{t_n})$  given by the diffusion bridge. To train the generator in the multistep regime, we use the same procedure as in one step except that to get input  $x_t$  for intermediate times  $t_n < t_N$ , we first perform inference of our generator to get  $x_0$  and then use bridge  $q(x_t|\tilde{x}_0, x_T)$ .

## 4. Related work

**Diffusion Bridge Models (DBMs) acceleration.** Unlike a wide scope of acceleration methods developed for classical diffusion and flow models, only a few approaches were developed for DBM acceleration. For the conditional DBMs, acceleration methods include more advanced samplers (Zheng et al., 2024; Wang et al., 2024) based on reformulated forward diffusion process as a non-markovian process inspired by Denoising Diffusion Implicit Models (Song et al., 2021). Also, there is a distillation method based on the distilling probability-flow ODE into a few steps using consistency models (He et al., 2024). However, for theoretical reasons (He et al., 2024, Section 3.4), consistency models for Diffusion Bridges cannot be distilled into one-step generators. Unlike these existing works, our method is applicable to both conditional and unconditional types of DBMs and can distill models into the one-step generator.

**Related diffusion and flow models distillation techniques.** Among the methods developed for the distillation of classical diffusion and flow models, the most related to our work are methods based on simultaneous training of few-step generators and auxiliary "fake" model, that predict score or drift function for the generator (Yin et al., 2024b;a; Zhou et al., 2024b; Huang et al., 2024). Unlike these approaches, we consider the distillation of Diffusion Bridge Models - the generalization of flow and diffusion models.

## 5. Experiments

This section highlights the applicability of our IBMD distillation method in both *unconditional* and *conditional* settings. To demonstrate this, we conducted experiments utilizing pretrained *unconditional* models used in I<sup>2</sup>SB paper (Liu et al., 2023a). Then we evaluated IBMD in *conditional*

### Algorithm 1 Inverse Bridge Matching Distillation (IBMD)

**Input** : Teacher network  $\hat{x}_0^* : \mathbb{R}^D \times [0, T] \times \mathbb{R}^D \rightarrow \mathbb{R}^D$ ;  
 Bridge  $q(x_t|x_0, x_T)$  used for training  $x^*$ ;  
 Generator network  $G_\theta : \mathbb{R}^D \times \mathbb{R}^D \rightarrow \mathbb{R}^D$ ;  
 Bridge network  $\hat{x}_0^\phi : \mathbb{R}^D \times [0, T] \times \mathbb{R}^D \rightarrow \mathbb{R}^D$ ;  
 Input distribution  $p(x_T)$  accessible by samples;  
 Weights function  $\lambda(t) : [0, T] \rightarrow \mathbb{R}^+$ ;  
 Batch size  $N$ ; Number of student iterations  $K$ ;  
 Number of bridge iterations  $L$ .

**Output** : Learned generator  $G_\theta$  of coupling  $p_\theta(x_0, x_T)$  for which Bridge Matching outputs drift  $v \approx v^*$ .

// Conditioning on  $x_T$  is used only for distillation of Conditional Bridge Matching models.

**for**  $k = 1$  **to**  $K$  **do**

**for**  $l = 1$  **to**  $L$  **do**

Sample batch  $x_T \sim p(x_T)$

Sample batch of noise  $z \sim \mathcal{N}(0, I)$

$x_0 \leftarrow G_\theta(x_T, z)$

Sample time batch  $t \sim U[0, T]$

Sample batch  $x_t \sim q(x_t|x_0, x_T)$

$\hat{\mathcal{L}}_\phi \leftarrow \frac{1}{N} \sum_{n=1}^N [\lambda(t) \|\hat{x}_0^\phi(x_t, t, x_T) - x_0\|^2]_n$

Update  $\phi$  by using  $\frac{\partial \hat{\mathcal{L}}_\phi}{\partial \phi}$

Sample batch  $x_T \sim p(x_T)$

Sample batch of noise  $z \sim \mathcal{N}(0, I)$

$x_0 \leftarrow G_\theta(x_T, z)$

Sample time batch  $t \sim U[0, T]$

Sample batch  $x_t \sim q(x_t|x_0, x_T)$

$\hat{\mathcal{L}}_\theta \leftarrow \frac{1}{N} \sum_{n=1}^N [\lambda(t) \|\hat{x}_0^*(x_t, t, x_T) - x_0\|^2 -$

$\lambda(t) \|\hat{x}_0^\phi(x_t, t, x_T) - x_0\|^2]_n$

Update  $\theta$  by using  $\frac{\partial \hat{\mathcal{L}}_\theta}{\partial \theta}$

settings using DDBM (Zhou et al., 2024a) setup (§5.2). For clarity, we denote our models as **IBMD-DDBM** and **IBMD-I<sup>2</sup>SB**, indicating that the teacher model is derived from DDBM or I<sup>2</sup>SB framework, respectively. We provide all the [technical details](#) in Appendix B.

### 5.1. Distillation of I2SB (5 setups)

Since known distillation and acceleration techniques are designed for the conditional models, there is no clear baseline for comparison. Thus, this section aims to demonstrate that our distillation technique significantly decreases NFE required to obtain the same quality of generation.

**Experimental Setup.** To test our approach for unconditional models, we consider models trained and published in I<sup>2</sup>SB paper (Liu et al., 2023a), specifically (a) two models for the 4x super-resolution with bicubic and pool kernels, (b) two models for JPEG restoration using quality factor QF= 5 and QF= 10, and (c) a model for center-inpainting with a center mask of size  $128 \times 128$  all of which were trained on ImageNet  $256 \times 256$  dataset (Deng et al., 2009).

Table 1. Results on the image super-resolution task. Baseline results are taken from I<sup>2</sup>SB (Liu et al., 2023a).

4× super-resolution (bicubic)	ImageNet (256 × 256)		
	NFE	FID ↓	CA ↑
DDRM (Kawar et al., 2022)	20	21.3	63.2
DDNM (Wang et al., 2023)	100	13.6	65.5
ΠGDM (Song et al., 2023)	100	3.6	72.1
ADM (Dhariwal & Nichol, 2021)	1000	14.8	66.7
CDSB (Shi et al., 2022)	50	13.6	61.0
I <sup>2</sup> SB (Liu et al., 2023a)	1000	2.8	70.7
<b>IBMD-I<sup>2</sup>SB (Ours)</b>	<b>1</b>	<b>2.5</b>	<b>72.4</b>

Table 2. Results on the image JPEG restoration task with QF=5. Baseline results are taken from I<sup>2</sup>SB (Liu et al., 2023a).

JPEG restoration, QF= 5.	ImageNet (256 × 256)		
	NFE	FID ↓	CA ↑
DDRM (Kawar et al., 2022)	20	28.2	53.9
ΠGDM (Song et al., 2023)	100	8.6	64.1
Palette (Saharia et al., 2022)	1000	8.3	64.2
CDSB (Shi et al., 2022)	50	38.7	45.7
I <sup>2</sup> SB (Liu et al., 2023a)	1000	<b>4.6</b>	67.9
I <sup>2</sup> SB (Liu et al., 2023a)	100	5.4	67.5
<b>IBMD-I<sup>2</sup>SB (Ours)</b>	<b>1</b>	<b>5.3</b>	<b>67.2</b>

For all the setups we use the same train part of ImageNet dataset, which was used to train the used models. For the evaluation we follow the same protocol used in the I<sup>2</sup>SB paper, i.e. use the full validation subset of ImageNet for super-resolution task and the 10'000 subset of validation for other tasks. We report the same FID (Heusel et al., 2017) and Classifier Accuracy (CA) using pre-trained ResNet50 model metrics used in the I<sup>2</sup>SB paper. We present our results in Table 1, Table 3, Table 2, Table 4 and Table 6. We provide the uncurated samples for all setups in Appendix C.

**Results.** For both super-resolution tasks (see Table 1, Table 3), our 1-step distilled model outperformed teacher model inference using all 1000 steps used in the training. Note that our model does not use the clean training target data  $p(x_0)$ , only the corrupted  $p(x_T)$ , hence this improvement is not due to additional training using paired data. We hypothesize that it is because the teacher model introduces approximation error during many steps of sampling, which may accumulate. For both JPEG restoration (see Table 2, Table 4), our 1-step distilled generator provides the quality of generation close to the teacher model and achieves around 100x time acceleration. For the inpainting problem (see Table 6), we present the results for 1, 2 and 4 steps distilled generator. Our 2 and 4-step generators provide a quality similar to the teacher I<sup>2</sup>SB model, in turn, there is still some gap for the 1-step model. These models provide around 5x time acceleration. We hypothesize that this setup is harder

Table 3. Results on the image super-resolution task. Baseline results are taken from I<sup>2</sup>SB (Liu et al., 2023a).

4× super-resolution (pool)	ImageNet (256 × 256)		
	NFE	FID ↓	CA ↑
DDRM (Kawar et al., 2022)	20	14.8	64.6
DDNM (Wang et al., 2023)	100	9.9	67.1
ΠGDM (Song et al., 2023)	100	3.8	72.3
ADM (Dhariwal & Nichol, 2021)	1000	3.1	73.4
CDSB (Shi et al., 2022)	50	13.0	61.3
I <sup>2</sup> SB (Liu et al., 2023a)	1000	2.7	71.0
<b>IBMD-I<sup>2</sup>SB (Ours)</b>	<b>1</b>	<b>2.6</b>	<b>72.7</b>

Table 4. Results on the image JPEG restoration task with QF=10. Baseline results are taken from I<sup>2</sup>SB (Liu et al., 2023a).

JPEG restoration, QF= 10.	ImageNet (256 × 256)		
	NFE	FID ↓	CA ↑
DDRM (Kawar et al., 2022)	20	16.7	64.7
ΠGDM (Song et al., 2023)	100	6.0	71.0
Palette (Saharia et al., 2022)	1000	5.4	70.7
CDSB (Shi et al., 2022)	50	18.6	60.0
I <sup>2</sup> SB (Liu et al., 2023a)	1000	<b>3.6</b>	72.1
I <sup>2</sup> SB (Liu et al., 2023a)	100	4.4	71.6
<b>IBMD-I<sup>2</sup>SB (Ours)</b>	<b>1</b>	<b>3.8</b>	<b>72.4</b>

for our model since it is required to generate the entire center fragment from scratch, while in other tasks, there is already some good approximation given by corrupted images.

## 5.2. Distillation of DDBM (3 setups)

This section addresses two primary objectives: (1) demonstrating the feasibility of conditional model distillation within our framework and (2) comparing with the CDBM (He et al., 2024) - a leading approach in Conditional Bridge Matching distillation, presented into different models: CBD (consistency distillation) and CBT (consistency training).

**Experimental Setup.** For evaluation, we use the same setups used in competing methods (He et al., 2024; Zheng et al., 2024). For the image-to-image translation task, we utilize the Edges→Handbags dataset (Isola et al., 2017) with a resolution of 64 × 64 pixels and the DIODE-Outdoor dataset (Vasiljevic et al., 2019) with a resolution of 256 × 256 pixels. For these tasks, we report FID and Inception Scores (IS) (Barratt & Sharma, 2018). For the image inpainting task, we use the same setup of center-inpainting as before.

**Results.** We utilized the same teacher model checkpoints and as in CDBM. We present the quantitative and qualitative results of IBMD on the image-to-image translation task in Table 5 and in Figures 12, 10 respectively. The competing methods, DBIM (Zhou et al., 2024a, Section 4.1) and CDBM (He et al., 2024, Section 3.4), cannot use single-step inference due to the singularity at the starting point  $x_T$ .

Table 5. Results on the Image-to-Image Translation Task (Training Sets). Methods are grouped by NFE ( $> 2, 2, 1$ ), with the best metrics bolded in each group. Baselines results are taken from CDBM.

	NFE	Edges $\rightarrow$ Handbags ( $64 \times 64$ )		DIODE-Outdoor ( $256 \times 256$ )	
		FID $\downarrow$	IS $\uparrow$	FID $\downarrow$	IS $\uparrow$
DDIB (Su et al., 2022)	$\geq 40$	186.84	2.04	242.3	4.22
SDEdit (Meng et al., 2021)	$\geq 40$	26.5	3.58	31.14	5.70
Rectified Flow (Liu et al., 2022a)	$\geq 40$	25.3	2.80	77.18	5.87
I <sup>2</sup> SB (Liu et al., 2023a)	$\geq 40$	7.43	3.40	9.34	5.77
DBIM (Zheng et al., 2024)	50	1.14	<b>3.62</b>	3.20	<b>6.08</b>
DBIM (Zheng et al., 2024)	100	<b>0.89</b>	<b>3.62</b>	<b>2.57</b>	6.06
CBD (He et al., 2024)		1.30	3.62	3.66	6.02
CBT (He et al., 2024)	2	0.80	3.65	<b>2.93</b>	<b>6.06</b>
IBMD-DDBM (Ours)		<b>0.67</b>	<b>3.69</b>	3.12	5.92
Pix2Pix (Isola et al., 2017)	1	74.8	<b>4.24</b>	82.4	4.22
IBMD-DDBM (Ours)		<b>1.26</b>	3.66	<b>4.07</b>	<b>5.89</b>

Table 6. Results on the Image Inpainting Task. Methods are grouped by NFE ( $> 4, 4, 2, 1$ ), with the best metrics bolded in each group. Baselines results are taken from CDBM.

Inpainting, Center ( $128 \times 128$ )	ImageNet ( $256 \times 256$ )		
	NFE	FID $\downarrow$	CA $\uparrow$
DDRM (Kawar et al., 2022)	20	24.4	62.1
IIGDM (Song et al., 2023)	100	7.3	<b>72.6</b>
DDNM (Wang et al., 2022)	100	15.1	55.9
Palette (Saharia et al., 2022)	1000	6.1	63.0
I <sup>2</sup> SB (Liu et al., 2023a)	10	5.4	65.97
DBIM (Zheng et al., 2024)	50	3.92	72.4
DBIM (Zheng et al., 2024)	100	<b>3.88</b>	<b>72.6</b>
CBD (He et al., 2024)		5.34	69.6
CBT (He et al., 2024)		4.77	70.3
IBMD-I <sup>2</sup> SB (Ours)	4	5.1	70.3
IBMD-DDBM (Ours)		<b>4.03</b>	<b>72.2</b>
CBD (He et al., 2024)		5.65	69.6
CBT (He et al., 2024)		5.34	69.8
IBMD-I <sup>2</sup> SB (Ours)	2	5.3	65.7
IBMD-DDBM (Ours)		<b>4.23</b>	<b>72.3</b>
IBMD-I <sup>2</sup> SB (Ours)		6.7	65.0
IBMD-DDBM (Ours)	1	<b>5.87</b>	<b>70.6</b>

We trained our IBMD with 1 and 2 NFEs on the Edges $\rightarrow$ Handbags dataset. We surpass CDBM at 2 NFE, outperform the teacher at 100 NFE, and achieve performance comparable to the teacher at 50 NFE with 1 NFE, resulting in a  $50\times$  acceleration. For the DIODE-Outdoor setup, we trained IBMD with 1 and 2 NFEs. We surpassed CBD in FID at 2 NFE, achieving results comparable to CBT with a slight drop in performance and maintaining strong performance at 1 NFE with minor quality reductions.

For image inpainting, Table 6 and Figure 9 show the quantitative and qualitative results of IBMD. We train IBMD with 4 NFE for image inpainting. It outperforms CBD and CBT at 4 NFE with a significant gap, surpassing both at 2 NFE and maintaining strong performance at 1 NFE while achieving teacher-level results at 50 NFE with a  $12.5\times$  speedup.

**Concerns regarding the evaluation protocol used in prior works.** For Edges-Handbags and DIODE-Outdoor setups, we follow the evaluation protocol originally introduced in DDBM (Zhou et al., 2024a) and later used in works on acceleration of DDBM (Zheng et al., 2024; He et al., 2024). For some reason, this protocol implies evaluation of the train set. Furthermore, test sets of these datasets consist of a tiny fraction of images (around several hundred), making the usage of standard metrics like FID challenging due to high statistical bias or variance of their estimation. Still, to assess the quality of the distilled model on the test sets, we provide the uncurated samples produced by our distill model and teacher model on these sets in Figures 13 and 11 in Appendix C. We also provide the uncurated samples on the train part in Figures 12 and 10 to compare models’ behavior on train and test sets. From these results, we see that the teacher model exhibits overfitting on both setups, e.g., it produces exactly the same images as corresponding reference images. In turn, on the test sets, teacher models work well for the handbag setups, while on the test set of DIODE images, it exhibits mode collapse and produces gray images. Nevertheless, our distilled model shows exactly the same behavior in both sets, i.e., our IBMD approach precisely distills the teacher model as expected.

## 6. Discussion

**Potential impact.** DBMs are used for data-to-data translation in different domains, including images, audio, and biological data. Our distillation technique provides a universal and efficient way to address the long inference of DBMs, making them more affordable in practice.

**Limitations.** Our method alternates between learning an additional bridge model and updating the student, which may be computationally expensive. Moreover, the student optimization requires backpropagation through the teacher, additional bridge, and the generator network, making it  $3\times$  time more memory expensive than training the teacher.



## Impact Statement

This paper presents work whose goal is to advance the field of Machine Learning. There are many potential societal consequences of our work, none which we feel must be specifically highlighted here.

## References

- Barratt, S. and Sharma, R. A note on the inception score. [arXiv preprint arXiv:1801.01973](#), 2018.
- De Bortoli, V., Liu, G.-H., Chen, T., Theodorou, E. A., and Nie, W. Augmented bridge matching. [arXiv preprint arXiv:2311.06978](#), 2023.
- Deng, J., Dong, W., Socher, R., Li, L.-J., Li, K., and Fei-Fei, L. Imagenet: A large-scale hierarchical image database. In [2009 IEEE conference on computer vision and pattern recognition](#), pp. 248–255. Ieee, 2009.
- Dhariwal, P. and Nichol, A. Diffusion models beat gans on image synthesis. [Advances in neural information processing systems](#), 34:8780–8794, 2021.
- Doob, J. L. and Doob, J. [Classical potential theory and its probabilistic counterpart](#), volume 262. Springer, 1984.
- Gushchin, N., Selikhanovych, D., Kholkin, S., Burnaev, E., and Korotin, A. Adversarial schrödinger bridge matching. [arXiv preprint arXiv:2405.14449](#), 2024.
- He, G., Zheng, K., Chen, J., Bao, F., and Zhu, J. Consistency diffusion bridge models. [arXiv preprint arXiv:2410.22637](#), 2024.
- Heusel, M., Ramsauer, H., Unterthiner, T., Nessler, B., and Hochreiter, S. Gans trained by a two time-scale update rule converge to a local nash equilibrium. [Advances in neural information processing systems](#), 30, 2017.
- Ho, J., Jain, A., and Abbeel, P. Denoising diffusion probabilistic models. [Advances in Neural Information Processing Systems](#), 33:6840–6851, 2020.
- Huang, Z., Geng, Z., Luo, W., and Qi, G.-j. Flow generator matching. [arXiv preprint arXiv:2410.19310](#), 2024.
- Isola, P., Zhu, J.-Y., Zhou, T., and Efros, A. A. Image-to-image translation with conditional adversarial networks. In [Proceedings of the IEEE conference on computer vision and pattern recognition](#), pp. 1125–1134, 2017.
- Kawar, B., Elad, M., Ermon, S., and Song, J. Denoising diffusion restoration models. [Advances in Neural Information Processing Systems](#), 35:23593–23606, 2022.
- Kong, Z., Shih, K. J., Nie, W., Vahdat, A., Lee, S.-g., Santos, J. F., Jukic, A., Valle, R., and Catanzaro, B. A2sb: Audio-to-audio schrödinger bridges. [arXiv preprint arXiv:2501.11311](#), 2025.
- Li, B., Xue, K., Liu, B., and Lai, Y.-K. Bbdm: Image-to-image translation with brownian bridge diffusion models. In [Proceedings of the IEEE/CVF conference on computer vision and pattern Recognition](#), pp. 1952–1961, 2023.
- Lipman, Y., Chen, R. T. Q., Ben-Hamu, H., Nickel, M., and Le, M. Flow matching for generative modeling. In [The Eleventh International Conference on Learning Representations](#), 2023. URL <https://openreview.net/forum?id=PqvMRDCJT9t>.
- Liu, G.-H., Vahdat, A., Huang, D.-A., Theodorou, E. A., Nie, W., and Anandkumar, A. I<sup>2</sup>sb: Image-to-image schrödinger bridge. [arXiv preprint arXiv:2302.05872](#), 2023a.
- Liu, X., Gong, C., et al. Flow straight and fast: Learning to generate and transfer data with rectified flow. In [The Eleventh International Conference on Learning Representations](#), 2022a.
- Liu, X., Wu, L., Ye, M., and qiang liu. Let us build bridges: Understanding and extending diffusion generative models. In [NeurIPS 2022 Workshop on Score-Based Methods](#), 2022b. URL <https://openreview.net/forum?id=0ef0CRKC9uZ>.
- Liu, X., Gong, C., and qiang liu. Flow straight and fast: Learning to generate and transfer data with rectified flow. In [The Eleventh International Conference on Learning Representations](#), 2023b. URL <https://openreview.net/forum?id=XVjTT1nw5z>.
- Meng, C., Song, Y., Song, J., Wu, J., Zhu, J.-Y., and Ermon, S. Sdedit: Image synthesis and editing with stochastic differential equations. [arXiv preprint arXiv:2108.01073](#), 2021.
- Pavon, M. and Wakolbinger, A. On free energy, stochastic control, and schrödinger processes. In [Modeling, Estimation and Control of Systems with Uncertainty: Proceedings of a Conference held in Sopron, Hungary, September 1990](#), pp. 334–348. Springer, 1991.
- Peluchetti, S. Diffusion bridge mixture transports, schrödinger bridge problems and generative modeling. [Journal of Machine Learning Research](#), 24(374):1–51, 2023a.
- Peluchetti, S. Non-denoising forward-time diffusions. [arXiv preprint arXiv:2312.14589](#), 2023b.

- Saharia, C., Chan, W., Chang, H., Lee, C., Ho, J., Salimans, T., Fleet, D., and Norouzi, M. Palette: Image-to-image diffusion models. In ACM SIGGRAPH 2022 conference proceedings, pp. 1–10, 2022.
- Shi, Y., De Bortoli, V., Deligiannidis, G., and Doucet, A. Conditional simulation using diffusion schrödinger bridges. In Uncertainty in Artificial Intelligence, pp. 1792–1802. PMLR, 2022.
- Shi, Y., Bortoli, V. D., Campbell, A., and Doucet, A. Diffusion schrödinger bridge matching. In Thirty-seventh Conference on Neural Information Processing Systems, 2023. URL <https://openreview.net/forum?id=qy070HsJT5>.
- Sohl-Dickstein, J., Weiss, E., Maheswaranathan, N., and Ganguli, S. Deep unsupervised learning using nonequilibrium thermodynamics. In International conference on machine learning, pp. 2256–2265. PMLR, 2015.
- Somnath, V. R., Pariset, M., Hsieh, Y.-P., Martinez, M. R., Krause, A., and Bunne, C. Aligned diffusion schrödinger bridges. In Uncertainty in Artificial Intelligence, pp. 1985–1995. PMLR, 2023.
- Song, J., Meng, C., and Ermon, S. Denoising diffusion implicit models. In International Conference on Learning Representations, 2021. URL <https://openreview.net/forum?id=StlgjarCHLP>.
- Song, J., Vahdat, A., Mardani, M., and Kautz, J. Pseudoinverse-guided diffusion models for inverse problems. In International Conference on Learning Representations, 2023.
- Su, X., Song, J., Meng, C., and Ermon, S. Dual diffusion implicit bridges for image-to-image translation. arXiv preprint arXiv:2203.08382, 2022.
- Tong, A. Y., Malkin, N., Fatras, K., Atanackovic, L., Zhang, Y., Hugué, G., Wolf, G., and Bengio, Y. Simulation-free schrödinger bridges via score and flow matching. In International Conference on Artificial Intelligence and Statistics, pp. 1279–1287. PMLR, 2024.
- Vargas, F., Thodoroff, P., Lamacraft, A., and Lawrence, N. Solving schrödinger bridges via maximum likelihood. Entropy, 23(9):1134, 2021.
- Vasiljevic, I., Kolkin, N., Zhang, S., Luo, R., Wang, H., Dai, F. Z., Daniele, A. F., Mostajabi, M., Basart, S., Walter, M. R., et al. Diode: A dense indoor and outdoor depth dataset. arXiv preprint arXiv:1908.00463, 2019.
- Wang, Y., Yu, J., and Zhang, J. Zero-shot image restoration using denoising diffusion null-space model. arXiv preprint arXiv:2212.00490, 2022.
- Wang, Y., Yu, J., and Zhang, J. Zero-shot image restoration using denoising diffusion null-space model. In The Eleventh International Conference on Learning Representations, 2023. URL <https://openreview.net/forum?id=mRieQgMtNTQ>.
- Wang, Y., Yoon, S., Jin, P., Tivnan, M., Song, S., Chen, Z., Hu, R., Zhang, L., Chen, Z., Wu, D., et al. Implicit image-to-image schrödinger bridge for image restoration. Zhiqiang and Wu, Dufan, Implicit Image-to-Image Schrödinger Bridge for Image Restoration, 2024.
- Yin, T., Gharbi, M., Park, T., Zhang, R., Shechtman, E., Durand, F., and Freeman, W. T. Improved distribution matching distillation for fast image synthesis. In The Thirty-eighth Annual Conference on Neural Information Processing Systems, 2024a. URL <https://openreview.net/forum?id=tQukGCDaNT>.
- Yin, T., Gharbi, M., Zhang, R., Shechtman, E., Durand, F., Freeman, W. T., and Park, T. One-step diffusion with distribution matching distillation. In Proceedings of the IEEE/CVF Conference on Computer Vision and Pattern Recognition, pp. 6613–6623, 2024b.
- Yue, Z., Wang, J., and Loy, C. C. Resshift: Efficient diffusion model for image super-resolution by residual shifting. Advances in Neural Information Processing Systems, 36, 2024.
- Zheng, K., He, G., Chen, J., Bao, F., and Zhu, J. Diffusion bridge implicit models. arXiv preprint arXiv:2405.15885, 2024.
- Zhou, L., Lou, A., Khanna, S., and Ermon, S. Denoising diffusion bridge models. arXiv preprint arXiv:2309.16948, 2023.
- Zhou, L., Lou, A., Khanna, S., and Ermon, S. Denoising diffusion bridge models. In The Twelfth International Conference on Learning Representations, 2024a. URL <https://openreview.net/forum?id=FKksTayvGo>.
- Zhou, M., Zheng, H., Wang, Z., Yin, M., and Huang, H. Score identity distillation: Exponentially fast distillation of pretrained diffusion models for one-step generation. In Forty-first International Conference on Machine Learning, 2024b.

## A. Proofs

Since all our theorems, propositions and proofs for the inverse Bridge Matching problems which is formulated for the already trained teacher model using some diffusion bridge, we assume all corresponding assumptions used in Bridge Matching. Extensive overview of them can be found in (Shi et al., 2023, Appendix C).

*Proof of Proposition 3.1.* Since both  $\text{BM}(\Pi_\theta)$  and  $M^*$  given by reverse-time SDE and the same distribution  $p_T(x_T)$  the KL-divergence expressed in the tractable form using the disintegration and Girsanov theorem (Vargas et al., 2021; Pavon & Wakolbinger, 1991):

$$\begin{aligned} \text{KL}(\text{BM}(\Pi_\theta) \| M^*) &= \mathbb{E}_{x_t, t} [g^2(t) \|v(x_t, t) - v^*(x_t, t)\|^2], \\ (x_0, x_T) &\sim p_\theta(x_0, x_T), t \sim U([0, T]), x_t \sim q(x_t | x_0, x_T). \end{aligned}$$

The expectation is taken over the marginal distribution  $p(x_t)$  of  $\Pi_\theta$  since it is the same as for  $\text{BM}(\Pi_\theta)$  (Shi et al., 2023, Proposition 2). In turn, the drift  $v(x_t, t)$  is the drift of Bridge Matching using  $\Pi_\theta$ , i.e.  $\text{BM}(\Pi_\theta)$ :

$$\begin{aligned} v &= \arg \min_{v'} \mathbb{E}_{x_t, t, x_0} [\|v'(x_t, t) - \nabla_{x_t} \log q(x_t | x_0)\|^2], \\ (x_0, x_T) &\sim p_\theta(x_0, x_T), t \sim U([0, T]), x_t \sim q(x_t | x_0, x_T). \end{aligned}$$

Combining this, the inverse problem can be expressed in a more tractable form:

$$\begin{aligned} \min_{\theta} \mathbb{E}_{x_t, t} [g^2(t) \|v(x_t, t) - v^*(x_t, t)\|^2], \quad \text{s.t.} & \quad (11) \\ v &= \arg \min_{v'} \mathbb{E}_{x_t, t, x_0} [\|v'(x_t, t) - \nabla_{x_t} \log q(x_t | x_0)\|^2] dt, \\ (x_0, x_T) &\sim p_\theta(x_0, x_T), t \sim U([0, T]), x_t \sim q(x_t | x_0, x_T). \end{aligned}$$

We can add positive valued weighting function  $\lambda(t)$  for the constraint:

$$v = \arg \min_{v'} \mathbb{E}_{x_t, t, x_0} [\lambda(t) \|v'(x_t, t) - \nabla_{x_t} \log q(x_t | x_0)\|^2] dt,$$

since it is the MSE regression and its solution is conditional expectation for any weights given by:

$$v(x_t, t) = \mathbb{E}_{x_0 | x_t, t} [\nabla_{x_t} \log q(x_t | x_0)].$$

We can add positive valued weighting function  $\lambda(t)$  for the main functional:

$$\mathbb{E}_{x_t, t} [\lambda(t) \|v(x_t, t) - v^*(x_t, t)\|^2],$$

since it does not change the optimum value (which is equal to 0) and optimal solution, which is the mixture of bridges with the same drift as the teacher model.  $\square$

*Proof of Theorem 3.2.* Consider inverse bridge matching optimization problem:

$$\begin{aligned} \min_{\theta} \mathbb{E}_{x_t, t} [\lambda(t) \|v(x_t, t) - v^*(x_t, t)\|^2], \quad \text{s.t.} & \quad (12) \\ v &= \arg \min_{v'} \mathbb{E}_{x_t, t, x_0} [\|v'(x_t, t) - \nabla_{x_t} \log q(x_t | x_0)\|^2], \\ (x_0, x_T) &\sim p_\theta(x_0, x_T), t \sim U([0, T]), x_t \sim q(x_t | x_0, x_T). \end{aligned}$$

First, note that since  $v = \arg \min_{v'} \mathbb{E}_{x_t, t, x_0} [\|v'(x_t, t) - \nabla_{x_t} \log q(x_t | x_0)\|^2]$ , i.e. minimizer of MSE functional it is given by conditional expectation as:

$$v(x_t, t) = \mathbb{E}_{x_0 | x_t, t} [\nabla_{x_t} \log q(x_t | x_0) | x_t, t]. \quad (13)$$

Then note that:

$$\min_{v'} \mathbb{E}_{x_t, t, x_0} [\lambda(t) \|v'(x_t, t) - \nabla_{x_t} \log q(x_t | x_0)\|^2] =$$

$$\begin{aligned}
 & \mathbb{E}_{x_t, t, x_0} [\lambda(t) \|v(x_t, t) - \nabla_{x_t} \log q(x_t|x_0)\|^2] = \\
 & \underbrace{\mathbb{E}_{x_t, t, x_0} [\lambda(t) \|v(x_t, t)\|^2]}_{\mathbb{E}_{x_t, t} [\lambda(t) \|v(x_t, t)\|^2]} - 2\mathbb{E}_{x_t, t, x_0} [\lambda(t) \langle v(x_t, t), \nabla_{x_t} \log q(x_t|x_0) \rangle] + \mathbb{E}_{x_t, t, x_0} [\lambda(t) \|\nabla_{x_t} \log q(x_t|x_0)\|^2] = \\
 & \mathbb{E}_{x_t, t} [\lambda(t) \|v(x_t, t)\|^2] - 2\mathbb{E}_{x_t, t} \left[ \lambda(t) \left\langle v(x_t, t), \underbrace{\mathbb{E}_{x_0|x_t, t} [\nabla_{x_t} \log q(x_t|x_0)]}_{=v(x_t, t)} \right\rangle \right] + \mathbb{E}_{x_t, t, x_0} [\lambda(t) \|\nabla_{x_t} \log q(x_t|x_0)\|^2] = \\
 & \mathbb{E}_{x_t, t} [\lambda(t) \|v(x_t, t)\|^2] - 2\mathbb{E}_{x_t, t} [\lambda(t) \|v(x_t, t)\|^2] + \mathbb{E}_{x_t, t, x_0} [\lambda(t) \|\nabla_{x_t} \log q(x_t|x_0)\|^2] = \\
 & -\mathbb{E}_{x_t, t} [\lambda(t) \|v(x_t, t)\|^2] + \mathbb{E}_{x_t, t, x_0} [\lambda(t) \|\nabla_{x_t} \log q(x_t|x_0)\|^2]. \tag{14}
 \end{aligned}$$

Hence, we derive that

$$\mathbb{E}_{x_t, t} [\lambda(t) \|v(x_t, t)\|^2] = \mathbb{E}_{x_t, t, x_0} [\lambda(t) \|\nabla_{x_t} \log q(x_t|x_0)\|^2] - \min_{v'} \mathbb{E}_{x_t, t, x_0} [\lambda(t) \|v'(x_t, t) - \nabla_{x_t} \log q(x_t|x_0)\|^2].$$

Now we use it to reformulate the initial objective:

$$\begin{aligned}
 & \mathbb{E}_{x_t, t} [\lambda(t) \|v(x_t, t) - v^*(x_t, t)\|^2] = \\
 & \mathbb{E}_{x_t, t} [\lambda(t) \|v(x_t, t)\|^2] - 2\mathbb{E}_{x_t, t} [\lambda(t) \langle v(x_t, t), v^*(x_t, t) \rangle] + \mathbb{E}_{x_t, t} [\lambda(t) \|v^*(x_t, t)\|^2] = \\
 & \underbrace{\mathbb{E}_{x_t, t, x_0} [\lambda(t) \|\nabla_{x_t} \log q(x_t|x_0)\|^2] - \min_{v'} \mathbb{E}_{x_t, t, x_0} [\lambda(t) \|v'(x_t, t) - \nabla_{x_t} \log q(x_t|x_0)\|^2]}_{=\mathbb{E}_{x_t, t} [\lambda(t) \|v(x_t, t)\|^2]} - \\
 & 2\mathbb{E}_{x_t, t} [\lambda(t) \langle v(x_t, t), v^*(x_t, t) \rangle] + \mathbb{E}_{x_t, t} [\lambda(t) \|v^*(x_t, t)\|^2] = \\
 & \mathbb{E}_{x_t, t, x_0} [\lambda(t) \|\nabla_{x_t} \log q(x_t|x_0)\|^2] - 2\mathbb{E}_{x_t, t} [\lambda(t) \langle v(x_t, t), v^*(x_t, t) \rangle] + \underbrace{\mathbb{E}_{x_t, t} [\lambda(t) \|v^*(x_t, t)\|^2]}_{\mathbb{E}_{x_t, t, x_0} [\lambda(t) \|v^*(x_t, t)\|^2]} - \\
 & \min_{v'} \mathbb{E}_{x_t, t, x_0} [\lambda(t) \|v'(x_t, t) - \nabla_{x_t} \log q(x_t|x_0)\|^2]
 \end{aligned}$$

Therefore, we get:

$$\begin{aligned}
 & \mathbb{E}_{x_t, t} [\lambda(t) \|v(x_t, t) - v^*(x_t, t)\|^2] = \\
 & \mathbb{E}_{x_t, t, x_0} [\lambda(t) \|\nabla_{x_t} \log q(x_t|x_0)\|^2] - 2\mathbb{E}_{x_t, t} [\lambda(t) \langle v(x_t, t), v^*(x_t, t) \rangle] + \mathbb{E}_{x_t, t, x_0} [\lambda(t) \|v^*(x_t, t)\|^2] - \\
 & \min_{v'} \mathbb{E}_{x_t, t, x_0} [\lambda(t) \|v'(x_t, t) - \nabla_{x_t} \log q(x_t|x_0)\|^2]
 \end{aligned}$$

To complete the proof, we use the relation  $v(x_t, t) = \mathbb{E}_{x_0|x_t, t} [\nabla_{x_t} \log q(x_t|x_0)|x_t, t]$  from Equation 13. Integrating these components, we arrive at the final result:

$$\begin{aligned}
 & \mathbb{E}_{x_t, t} [\lambda(t) \|v(x_t, t) - v^*(x_t, t)\|^2] = \\
 & \mathbb{E}_{x_t, t, x_0} [\lambda(t) \|\nabla_{x_t} \log q(x_t|x_0)\|^2] - 2\mathbb{E}_{x_t, t} [\lambda(t) \langle \mathbb{E}_{x_0|x_t, t} [\nabla_{x_t} \log q(x_t|x_0)|x_t, t], v^*(x_t, t) \rangle] + \mathbb{E}_{x_t, t, x_0} [\lambda(t) \|v^*(x_t, t)\|^2] - \\
 & \min_{v'} \mathbb{E}_{x_t, t, x_0} [\lambda(t) \|v'(x_t, t) - \nabla_{x_t} \log q(x_t|x_0)\|^2] = \\
 & \mathbb{E}_{x_t, t, x_0} [\lambda(t) \|\nabla_{x_t} \log q(x_t|x_0)\|^2] - 2\mathbb{E}_{x_t, t, x_0} [\lambda(t) \langle \nabla_{x_t} \log q(x_t|x_0), v^*(x_t, t) \rangle] + \mathbb{E}_{x_t, t, x_0} [\lambda(t) \|v^*(x_t, t)\|^2] - \\
 & \min_{v'} \mathbb{E}_{x_t, t, x_0} [\lambda(t) \|v'(x_t, t) - \nabla_{x_t} \log q(x_t|x_0)\|^2] = \\
 & \mathbb{E}_{x_t, t, x_0} [\lambda(t) \|v^*(x_t, t) - \nabla_{x_t} \log q(x_t|x_0)\|^2] - \min_{v'} \mathbb{E}_{x_t, t, x_0} [\lambda(t) \|v'(x_t, t) - \nabla_{x_t} \log q(x_t|x_0)\|^2].
 \end{aligned}$$

□

*Proof of Proposition 3.3.* Consider the problem from Proposition 3.2:

$$\min_{\theta} \left[ \mathbb{E}_{x_t, t, x_0} [\lambda(t) \|v^*(x_t, t) - \nabla_{x_t} \log q(x_t|x_0)\|^2] - \min_{\phi} \mathbb{E}_{x_t, t, x_0} [\lambda(t) \|v_{\phi}(x_t, t) - \nabla_{x_t} \log q(x_t|x_0)\|^2] \right],$$

For the priors with the drift  $f(t)x$  the regression target is  $\nabla_{x_t} \log q(x_t|x_0) = -\frac{x_t - \alpha_t x_0}{\sigma_t^2}$ . Hence one can use the parametrization  $v(x_t, t) = -\frac{x_t - \alpha_t \hat{x}_0^*(x_t, t)}{\sigma_t^2}$ . We use reparameterization of both  $v^*$  and  $v_\phi$  given by:

$$v^*(x_t, t) = -\frac{x_t - \alpha_t \hat{x}_0^*(x_t, t)}{\sigma_t^2}, \quad v_\phi(x_t, t) = -\frac{x_t - \alpha_t \hat{x}_0^\phi(x_t, t)}{\sigma_t^2}$$

and get:

$$\begin{aligned} & \min_{\theta} \left[ \mathbb{E}_{x_t, t, x_0} [\lambda(t) \|v^*(x_t, t) - \nabla_{x_t} \log q(x_t|x_0)\|^2] - \min_{\phi} \mathbb{E}_{x_t, t, x_0} [\lambda(t) \|v_\phi(x_t, t) - \nabla_{x_t} \log q(x_t|x_0)\|^2] \right] = \\ & \min_{\theta} \left[ \underbrace{\mathbb{E}_{x_t, t, x_0} \left[ \lambda(t) \frac{\alpha_t^2}{\sigma_t^4} \|\hat{x}_0^*(x_t, t) - x_0\|^2 \right]}_{\stackrel{\text{def}}{=} \lambda'(t)} - \min_{\phi} \mathbb{E}_{x_t, t, x_0} \left[ \lambda(t) \frac{\alpha_t^2}{\sigma_t^4} \|\hat{x}_0^\phi(x_t, t) - x_0\|^2 \right]}_{\stackrel{\text{def}}{=} \lambda'(t)} \right] = \\ & \min_{\theta} \left[ \mathbb{E}_{x_t, t, x_0} [\lambda'(t) \|\hat{x}_0^*(x_t, t) - x_0\|^2] - \min_{\phi} \mathbb{E}_{x_t, t, x_0} [\lambda'(t) \|\hat{x}_0^\phi(x_t, t) - x_0\|^2] \right], \end{aligned}$$

where  $\lambda'(t)$  is just another positive weighting function. □

*Proof of Theorem 3.4.* In a fully analogical way, as for the unconditional case we consider the set of the Inverse Bridge Matching problems indexes by  $x_T$ :

$$\left\{ \min_{\theta} [\text{KL}(\text{BM}(\Pi_{\theta|x_T}) || M_{x_T}^*)] \right\}_{x_T},$$

where  $M_{x_T}^*$  is a result of Bridge Matching conditioned on  $x_T$  and  $\Pi_{\theta|x_T}$  is a Mixture of Bridges for each  $x_T$  constructed using bridge  $q(x_t|x_0, x_T)$  and coupling  $p_{\theta}(x_0|x_T)\delta_{x_T}(x)$ .

By employing the same reasoning as in the proof of Proposition 3.1, the inverse problem can be reformulated as follows:

$$\begin{aligned} & \min_{\theta} \mathbb{E}_{x_t, t, x_T} [g^2(t) \|v(x_t, t, x_T) - v^*(x_t, t, x_T)\|^2], \quad \text{s.t.} \\ & v = \arg \min_{v'} \mathbb{E}_{x_t, t, x_0, x_T} [\|v'(x_t, t, x_T) - \nabla_{x_t} \log q(x_t|x_0)\|^2] dt, \\ & (x_0, x_T) \sim p_{\theta}(x_0, x_T), \quad t \sim U([0, T]), \quad x_t \sim q(x_t|x_0, x_T). \end{aligned}$$

Following the proof of Theorem 3.2, we obtain a tractable formulation incorporating a weighting function:

$$\begin{aligned} & \min_{\theta} \left[ \mathbb{E}_{x_t, t, x_0, x_T} [\lambda(t) \|v^*(x_t, t, x_T) - \nabla_{x_t} \log q(x_t|x_0)\|^2] - \right. \\ & \left. \min_{\phi} \mathbb{E}_{x_t, t, x_0, x_T} [\lambda(t) \|v_\phi(x_t, t, x_T) - \nabla_{x_t} \log q(x_t|x_0)\|^2] \right]. \end{aligned}$$

Utilizing the reparameterization under additional conditions (§2.3), we obtain the following representations:

$$v^*(x_t, t, x_T) = -\frac{x_t - \alpha_t \hat{x}_0^*(x_t, t, x_T)}{\sigma_t^2}, \quad v_\phi(x_t, t, x_T) = -\frac{x_t - \alpha_t \hat{x}_0^\phi(x_t, t, x_T)}{\sigma_t^2}.$$

Consequently, applying the proof technique from Proposition 3.3, we derive the final expression:

$$\begin{aligned} & \min_{\theta} \left[ \mathbb{E}_{x_t, t, x_0} [\lambda(t) \|\hat{x}_0^*(x_t, t, x_T) - x_0\|^2] - \min_{\phi} \mathbb{E}_{x_t, t, x_0} [\lambda(t) \|\hat{x}_0^\phi(x_t, t, x_T) - x_0\|^2] \right], \\ & (x_0, x_T) \sim p_{\theta}(x_0, x_T), \quad t \sim U([0, T]), \quad x_t \sim q(x_t|x_0, x_T). \end{aligned}$$

□

## B. Experimental details

All hyperparameters are listed in Table 7. We used batch size 256 and ema decay 0.99 for setups. For each setup, we started the student and bridge networks using checkpoints from the teacher models. In setups where the model adapts to noise: (1) We added extra layers for noise inputs (set to zero initially), (2) Noise was concatenated with input data before input it to the network. Datasets, code sources, and licenses are included in Table 8.

## Inverse Bridge Matching Distillation

Task	Dataset	Teacher	NFE	$L/K$ ratio	LR	Grad Updates	Noise
4× super-resolution (bicubic)	ImageNet	I <sup>2</sup> SB	1	5:1	5e-5	3000	✓
4× super-resolution (pool)	ImageNet	I <sup>2</sup> SB	1	5:1	5e-5	3000	✓
JPEG restoration, QF = 5	ImageNet	I <sup>2</sup> SB	1	5:1	5e-5	2000	✓
JPEG restoration, QF = 10	ImageNet	I <sup>2</sup> SB	1	5:1	5e-5	3000	✓
Center-inpainting (128 × 128)	ImageNet	I <sup>2</sup> SB	4	5:1	5e-5	2000	✗
Sketch to Image	Edges → Handbags	DDBM	2	5:1	1e-5	300	✓
Sketch to Image	Edges → Handbags	DDBM	1	5:1	1e-5	14000	✓
Normal to Image	DIODE-Outdoor	DDBM	2	5:1	1e-5	500	✓
Normal to Image	DIODE-Outdoor	DDBM	1	5:1	1e-5	3700	✓
Center-inpainting (128 × 128)	ImageNet	DDBM	4	1:1	3e-6	3000	✓

Table 7. Table entries specify experimental configurations: *NFE* indicates multistep training (Sec. §3.5); *L/K* represents bridge/student gradient iteration ratios (Alg. §3.4); *Grad Updates* shows student gradient steps; *Noise* notes stochastic pipeline incorporation.

Table 8. The used datasets, codes and their licenses.

Name	URL	Citation	License
Edges→Handbags	<a href="#">GitHub Link</a>	(Isola et al., 2017)	BSD
DIODE-Outdoor	<a href="#">Dataset Link</a>	(Vasiljevic et al., 2019)	MIT
ImageNet	<a href="#">Website Link</a>	(Deng et al., 2009)	\
Guided-Diffusion	<a href="#">GitHub Link</a>	(Dhariwal & Nichol, 2021)	MIT
I <sup>2</sup> SB	<a href="#">GitHub Link</a>	(Liu et al., 2023a)	CC-BY-NC-SA-4.0
DDBM	<a href="#">GitHub Link</a>	(Zhou et al., 2023)	\
DBIM	<a href="#">GitHub Link</a>	(Zheng et al., 2024)	\

### B.1. Distillation of I<sup>2</sup>SB models.

We extended the I<sup>2</sup>SB repository (see Table 8), integrating our distillation framework. The following sections outline the setups, adapted following the I<sup>2</sup>SB.

**Multistep implementation** In this setup, we use the student model’s full inference process during multistep training (Section 3.5). This means that  $x_0$  is generated with inferenced of the model  $G_\theta$  through *all* timesteps ( $T = t_N, \dots, t_1 = 0$ ) in the multistep sequence. The generated  $x_0$  is subsequently utilized in the computation of the bridge  $\hat{\mathcal{L}}_\phi$  or student  $\hat{\mathcal{L}}_\theta$  objective functions, as formalized in Algorithm 1.

**4× super-resolution.** Our implementation of the degradation operators aligns with the filters implementation proposed in DDRM (Kawar et al., 2022). Firstly, we synthesize images at  $64 \times 64$  resolution, then upsample them to  $256 \times 256$  to ensure dimensional consistency between clean and degraded inputs. For evaluation, we follow established benchmarks (Saharia et al., 2022; Song et al., 2023) by computing the FID on reconstructions from the full ImageNet validation set, with comparisons drawn against the training set statistics.

**JPEG restoration.** Our JPEG degradation implementation, employing two distinct quality factors (QF=5, QF=10), follows (Kawar et al., 2022). FID is evaluated on a 10,000-image ImageNet [validation subset](#) against the full validation set’s statistics, following baselines (Saharia et al., 2022; Song et al., 2023).

**Inpainting.** For the image inpainting task on ImageNet at  $256 \times 256$  resolution, we utilize a fixed  $128 \times 128$  centrally positioned mask, aligning with the methodologies of DBIM (Zheng et al., 2024) and CDBM (He et al., 2024). During training, the model is trained only on the masked regions, while during generation, the unmasked areas are deterministically retained from the initial corrupted image  $x_T$  to preserve structural fidelity of unmasked part of images. We trained the model with 4 NFEs via the multistep method (Section 3.5) and tested it with 1, 2, and 4 NFEs.

### B.2. Distillation of DDBM models.

We extended the DDBM repository (Table 8) by integrating our distillation framework. Subsequent sections outline the experimental setups, adapted from the DDBM (Zheng et al., 2024).

**Multistep implementation** In this setup, the multistep training (Section 3.5) adopts the methodology of DMD (Yin et al., 2024a), wherein a timestep  $t$  is uniformly sampled from the predefined sequence  $(t_1, \dots, t_N)$ . The model  $G_\theta$  then generates

$x_0$  by iteratively reversing the process from the terminal timestep  $t_N = T$  to the sampled intermediate timestep  $t$ . This generated  $x_0$  is subsequently used to compute the bridge network’s loss  $\widehat{\mathcal{L}}_\phi$  or the student network’s loss  $\widehat{\mathcal{L}}_\theta$ , as detailed in Algorithm 1.

**Edges  $\rightarrow$  Handbags** The model was trained utilizing the Edges $\rightarrow$ Handbags image-to-image translation task (Isola et al., 2017), with the  $64 \times 64$  resolution images. Two versions were trained under the multistep regime (Section 3.5), with 2 and 1 NFEs during training. Both models were evaluated using the same NFE to match training settings.

**DIODE-Outdoor** Following prior work (Zhou et al., 2023; Zheng et al., 2024; He et al., 2024), we used the DIODE outdoor dataset, preprocessed via the DBIM repository’s script for training/test sets (Table 8). Two versions were trained under the multistep regime (Section 3.5), with 2 and 1 NFEs during training. Both models were evaluated using the same NFE to match training settings.

**Inpainting** All setups matched those in Section B.1 inpainting, except we use a CBDM checkpoint (Zheng et al., 2024). This checkpoint is adjusted by the authors to: (1) condition on  $x_T$  and (2) ImageNet class labels as input to guide the model. Also this is the same checkpoint used in both CDBM (He et al., 2024) and DBIM (Zheng et al., 2024) works.

### C. Additional results

### Inverse Bridge Matching Distillation

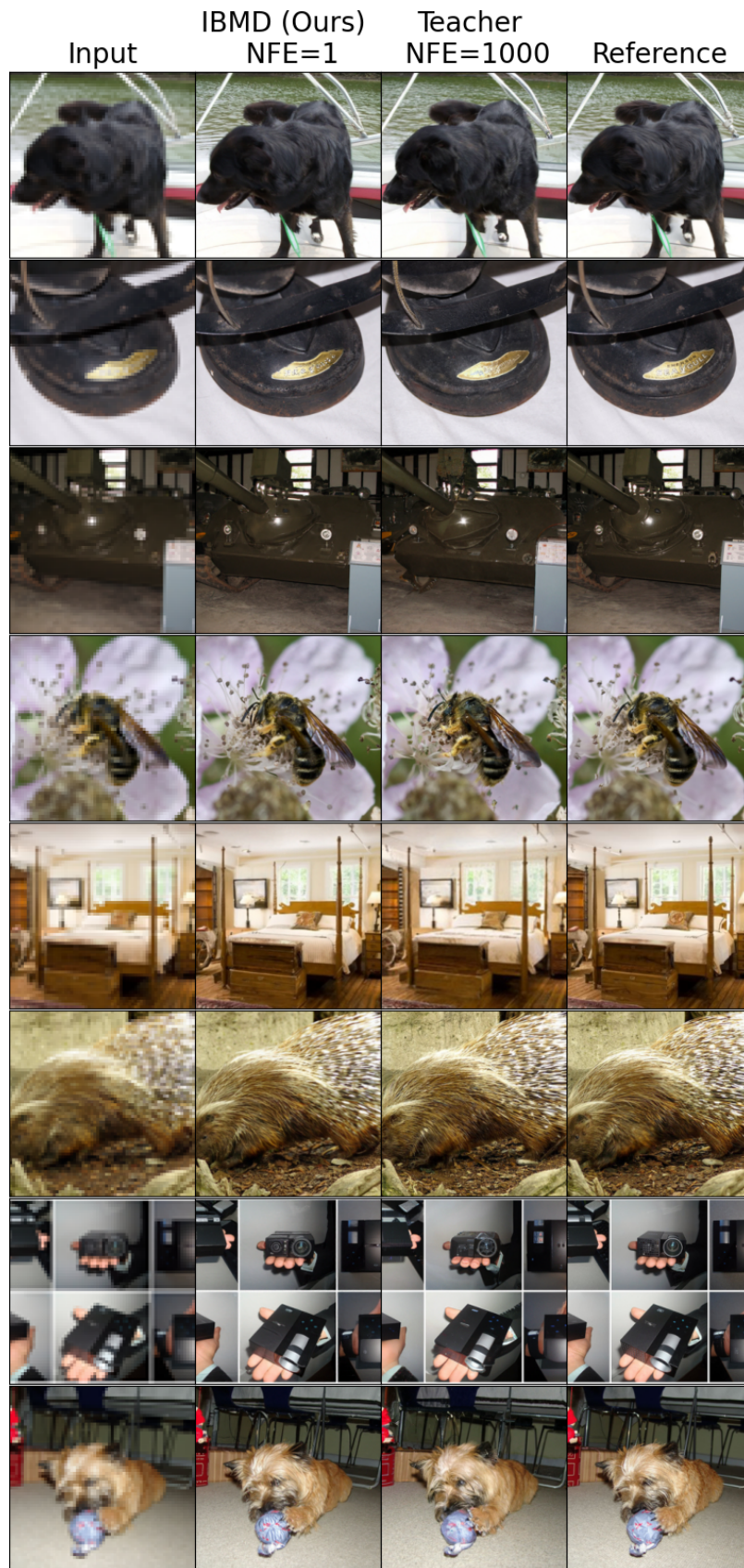


Figure 4. Uncurated samples for IBMD- $I^2$ SB distillation of 4x-super-resolution with bicubic kernel on ImageNet  $256 \times 256$  images.



Inverse Bridge Matching Distillation

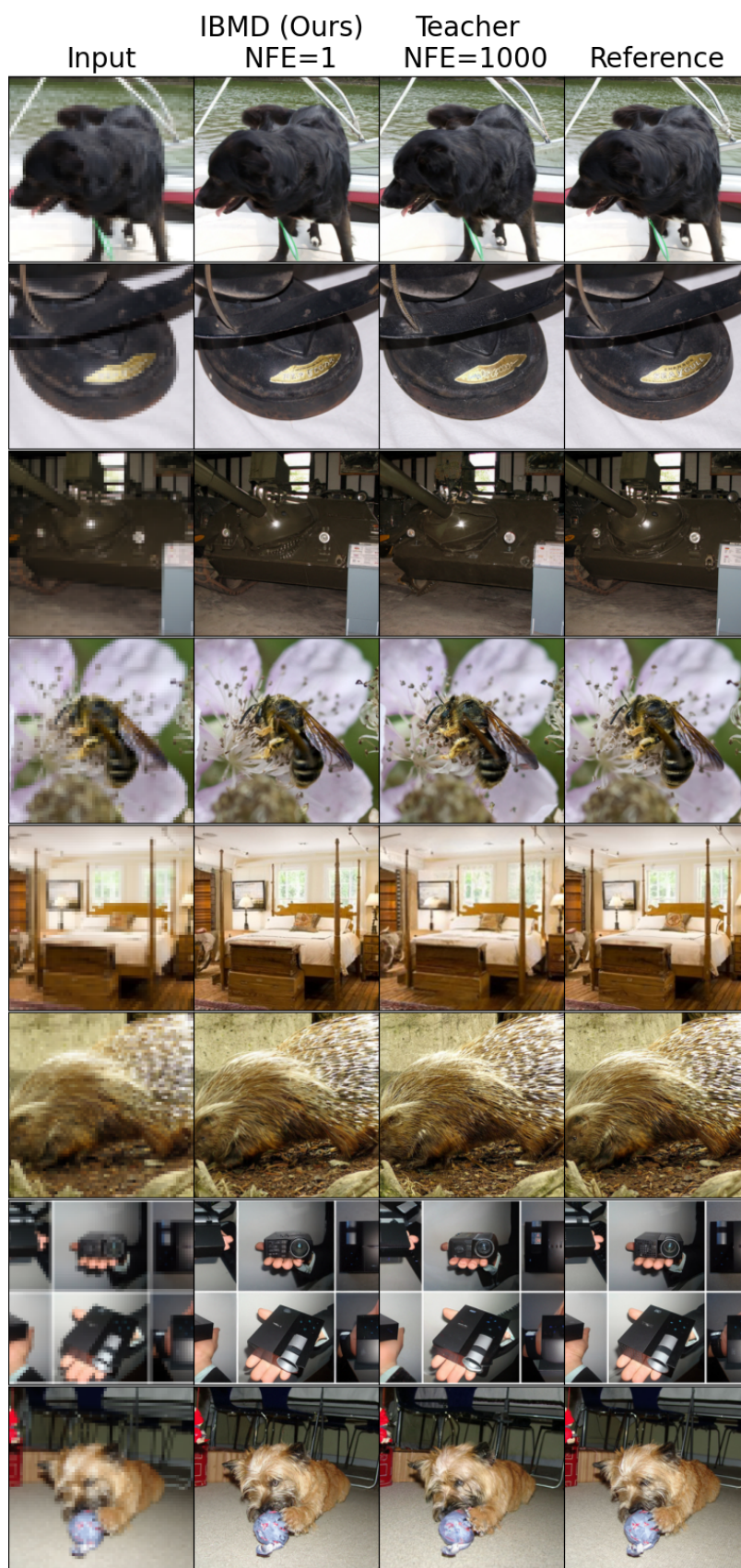


Figure 5. Uncurated samples for IBMD- $I^2$ SB distillation of 4x-super-resolution with pool kernel on ImageNet  $256 \times 256$  images.

### Inverse Bridge Matching Distillation

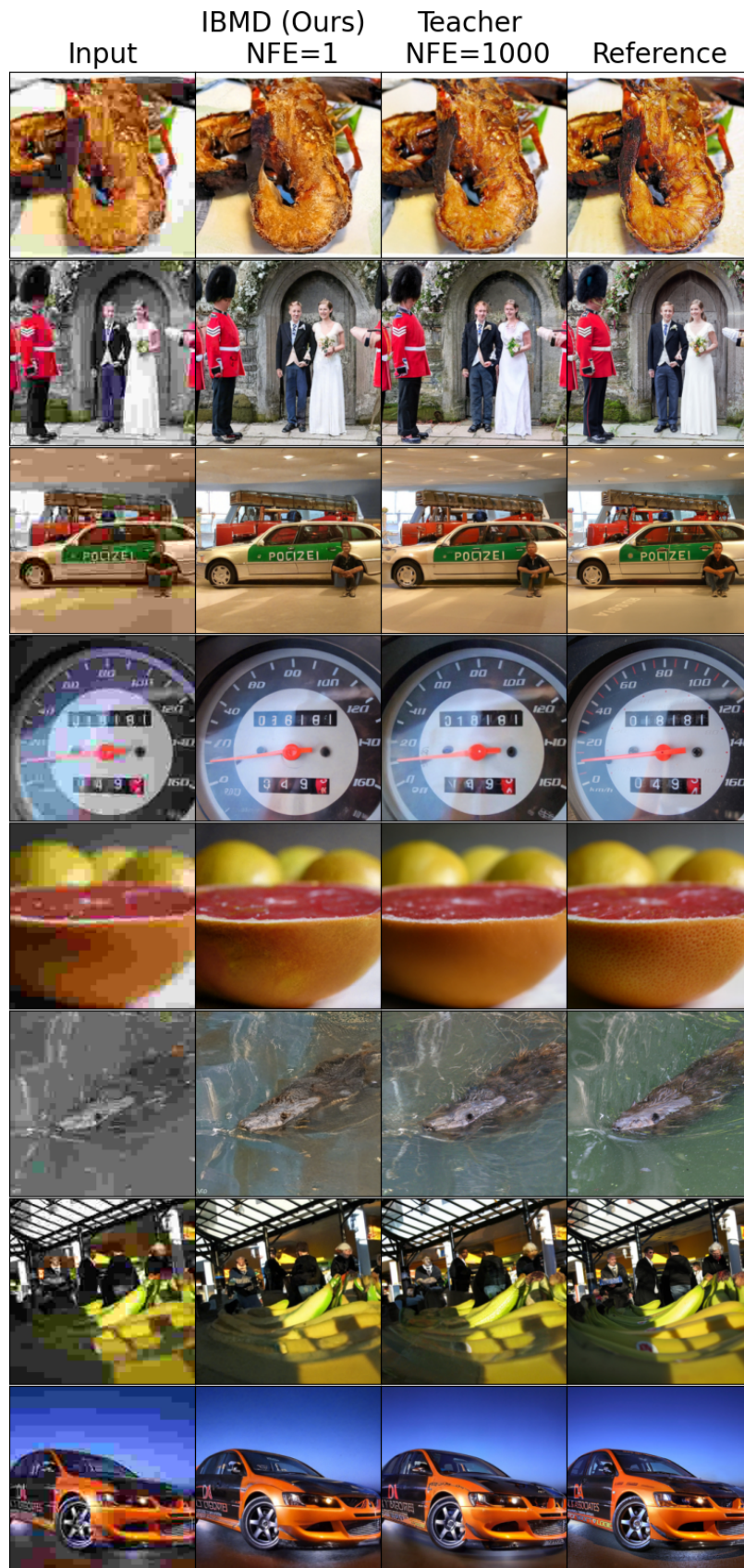


Figure 6. Uncurated samples for IBMD- $I^2$ SB distillation of Jpeg restoration with QF=5 on ImageNet  $256 \times 256$  images.

Inverse Bridge Matching Distillation



Figure 7. Uncurated samples for IBMD-I<sup>2</sup>SB distillation of Jpeg restoration with QF=10 on ImageNet 256 × 256 images.

Inverse Bridge Matching Distillation



Figure 8. Uncurated samples for IBMD-I2SB distillation trained for inpainting with NFE= 4 and inferred with different inference NFE on ImageNet 256 × 256 images.

**Inverse Bridge Matching Distillation**

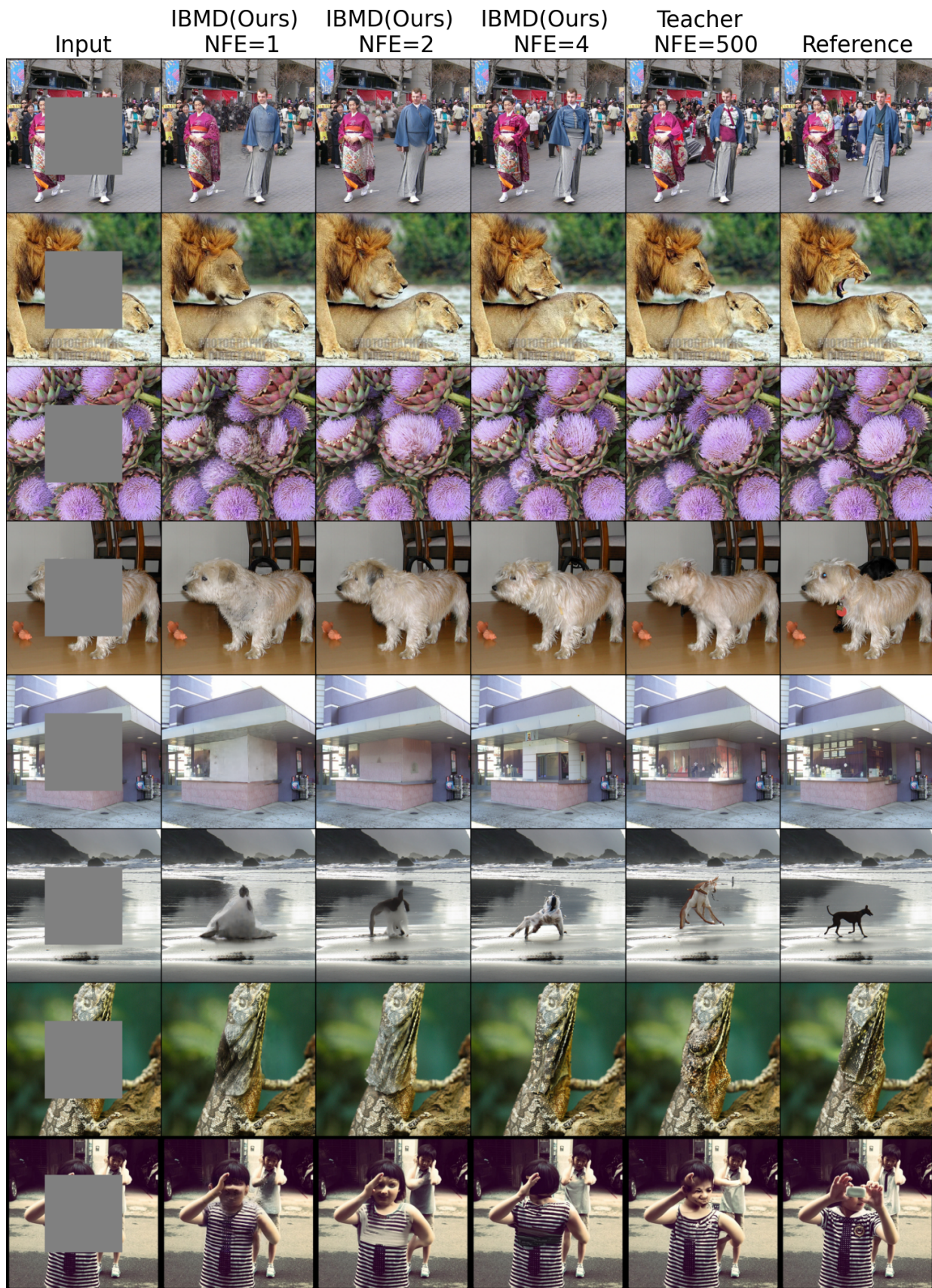


Figure 9. Uncurated samples for IBMD-DDBM distillation trained for inpainting with NFE= 4 and inferred with different inference NFE on ImageNet  $256 \times 256$  images.

### Inverse Bridge Matching Distillation

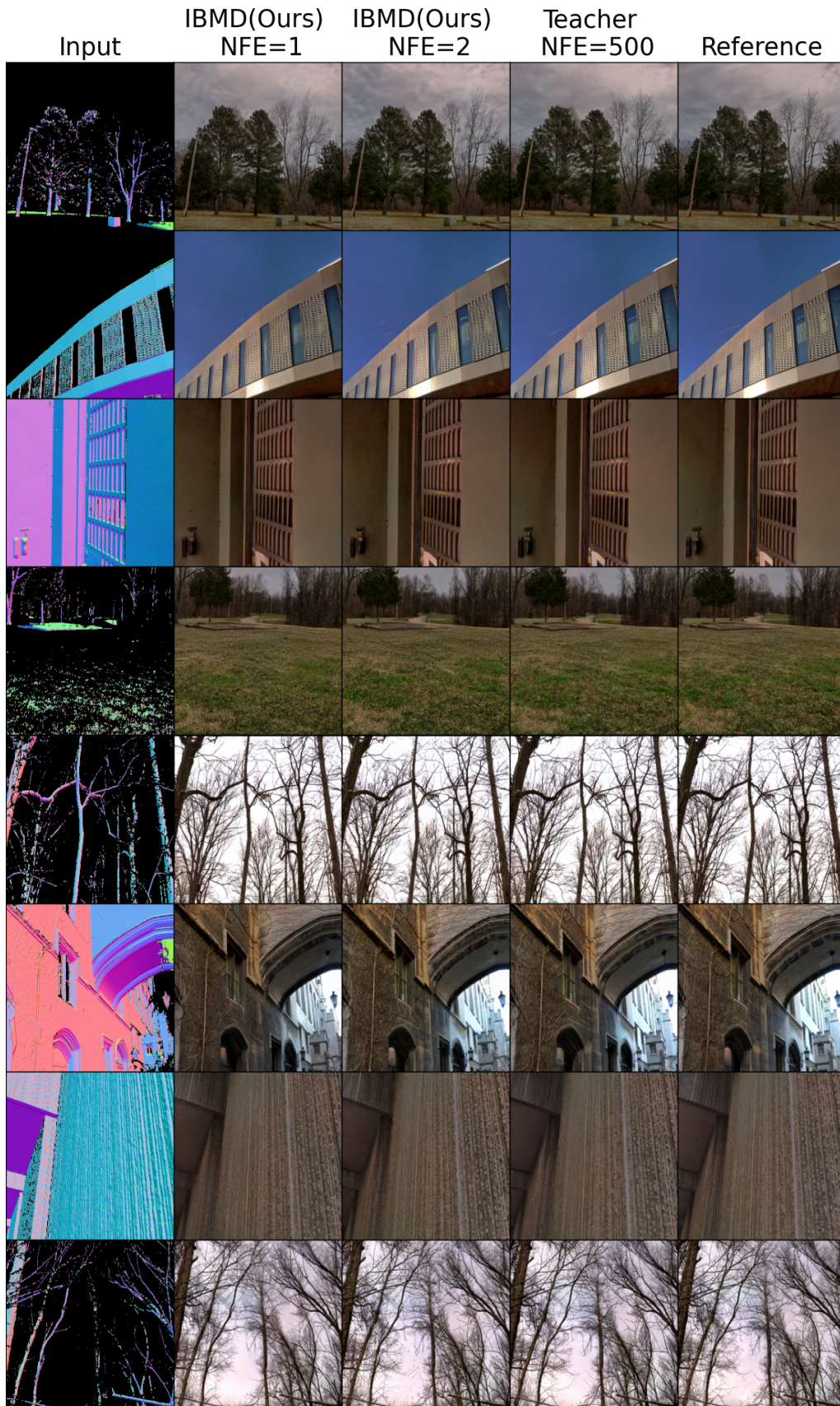


Figure 10. Uncurated samples from IBMD-DDBM distillation trained on the DIODE-Outdoor dataset ( $256 \times 256$ ) with NFE= 2 and NFE= 1, inferred using the corresponding NFEs on the training set.

Inverse Bridge Matching Distillation

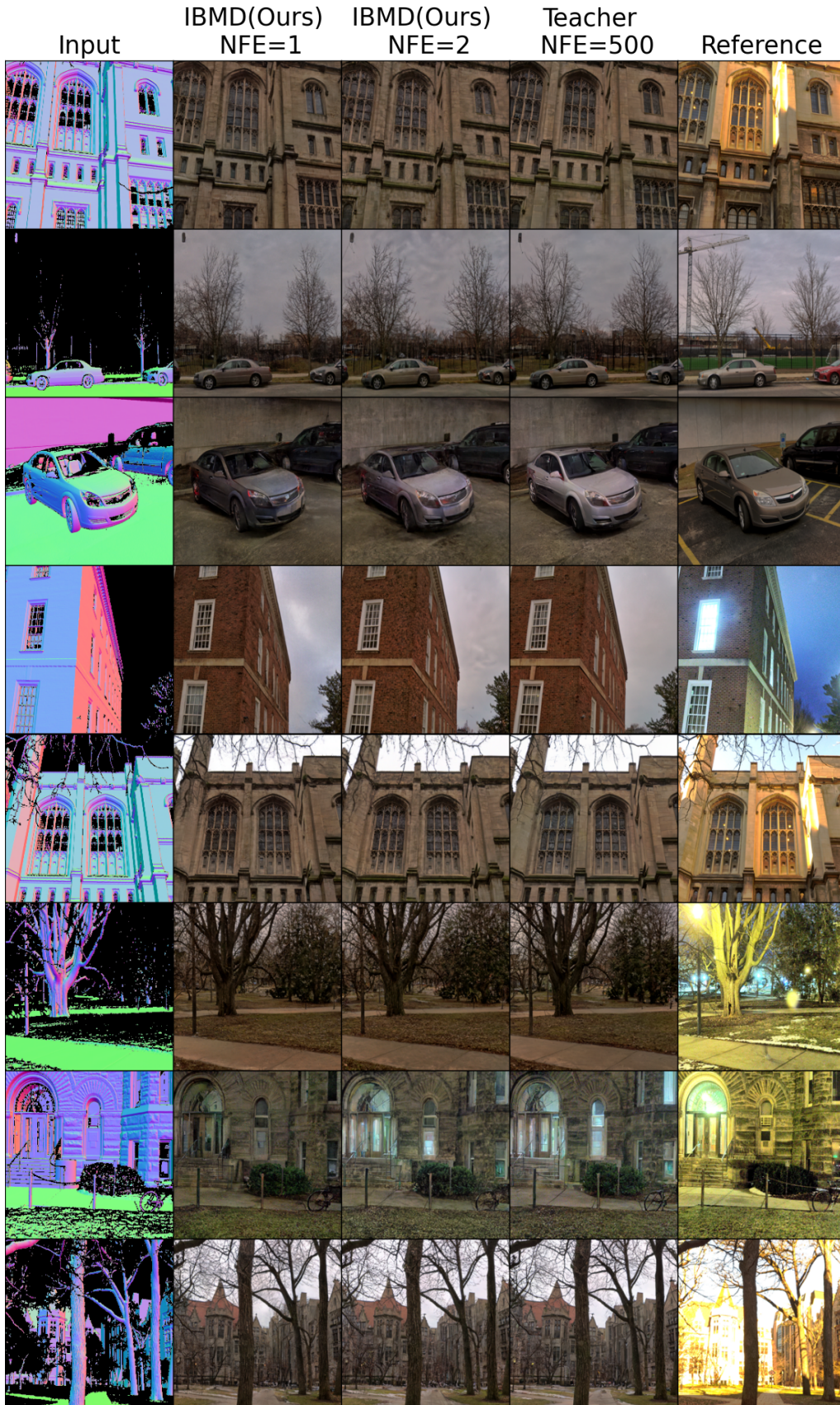


Figure 11. Uncurated samples from IBMD-DDBM distillation trained on the DIODE-Outdoor dataset ( $256 \times 256$ ) with NFE= 2 and NFE= 1, inferred using the corresponding NFEs on the test set.

**Inverse Bridge Matching Distillation**

Input	IBMD(Ours) NFE=1	IBMD(Ours) NFE=2	Teacher NFE=500	Reference

Figure 12. Uncurated samples from IBMD-DDBM distillation trained on the Edges  $\rightarrow$  Handbags dataset ( $64 \times 64$ ) with NFE= 2 and NFE= 1, inferred using the corresponding NFEs on the training set.<sub>24</sub>



Inverse Bridge Matching Distillation



Figure 13. Uncurated samples from IBMD-DDBM distillation trained on the Edges  $\rightarrow$  Handbags dataset ( $64 \times 64$ ) with NFE= 2 and NFE= 1, inferred using the corresponding NFEs on the test set.